



Article

Quantifying Water Consumption through the Satellite Estimation of Land Use/Land Cover and Groundwater Storage Changes in a Hyper-Arid Region of Egypt

Ayihumaier Halipu ^{1,*}, Xuechen Wang ¹, Erina Iwasaki ² , Wei Yang ^{1,3} and Akihiko Kondoh ^{1,3}

¹ Graduate School of Science and Engineering, Chiba University, Chiba 263-8522, Japan; casa6077@chiba-u.jp (X.W.); yangwei@chiba-u.jp (W.Y.); kondoh@faculty.chiba-u.jp (A.K.)

² Faculty of Foreign Studies, Sophia University, Tokyo 102-8554, Japan; iwasaki@sophia.ac.jp

³ Center for Environmental Remote Sensing, Chiba University, Chiba 263-8522, Japan

* Correspondence: ayxa6085@chiba-u.jp

Abstract: One of the areas that show the most visible effects of human-induced land alterations is also the world's most essential resource: water. Decision-makers in arid regions face considerable difficulties in providing and maintaining sustainable water resource management. However, developing appropriate and straightforward approaches for quantifying water use in arid/hyper-arid regions is still a formidable challenge. Meanwhile, a better knowledge of the effects of land use land cover (LULC) changes on natural resources and environmental systems is required. The purpose of this study was to quantify the water consumption in a hyper-arid region (New Valley, Egypt) using two different approaches—LULC based on optical remote sensing data and groundwater storage changes based on Gravity Recovery Climate Experiment (GRACE) satellite data—and to compare and contrast the quantitative results of the two approaches. The LULC of the study area was constructed from 1986 to 2021 to identify the land cover changes and investigate the primary water consumption patterns. The analysis of groundwater storage changes utilized two GRACE mascon solutions from 2002 to 2021 in New Valley. The results showed an increase in agricultural areas in New Valley's oases. They also showed an increased in irrigation water usage and a continuous decrease in the groundwater storage of New Valley. The overall water usage in New Valley for domestic and irrigation was calculated as 18.62 km³ (0.93 km³/yr) based on the LULC estimates. Moreover, the groundwater storage changes of New Valley were extracted using GRACE and calculated to be 19.36 ± 7.96 km³ (0.97 ± 0.39 km³/yr). The results indicated that the water use calculated from LULC was consistent with the depletion in groundwater storage calculated by applying GRACE. This study provides an essential reference for regional sustainability and water resource management in arid/hyper-arid regions.

Keywords: arid region; LULC; water consumption; GRACE; sustainability



Citation: Halipu, A.; Wang, X.; Iwasaki, E.; Yang, W.; Kondoh, A. Quantifying Water Consumption through the Satellite Estimation of Land Use/Land Cover and Groundwater Storage Changes in a Hyper-Arid Region of Egypt. *Remote Sens.* **2022**, *14*, 2608. <https://doi.org/10.3390/rs14112608>

Academic Editor: Gabriel Senay

Received: 2 April 2022

Accepted: 27 May 2022

Published: 29 May 2022

Publisher's Note: MDPI stays neutral with regard to jurisdictional claims in published maps and institutional affiliations.



Copyright: © 2022 by the authors. Licensee MDPI, Basel, Switzerland. This article is an open access article distributed under the terms and conditions of the Creative Commons Attribution (CC BY) license (<https://creativecommons.org/licenses/by/4.0/>).

1. Introduction

New Valley is the largest governorate in Egypt and represents 46% of Egypt's area, comprising about 440,098 km². It includes the Dakhla, Kharga, and Farafra oases, which are linked to each other. The population of New Valley has quadrupled from 1960 to 2020, with an increase from 34,000 in 1960 [1] to 141,774 in 1996 [2] to 257,752 in 2021 [3], representing about 0.3% of the national total. The annual population growth rate in New Valley is 2.6, higher than the national rate of 1.9 [4].

New Valley, as a significant agricultural society, has various industries that are of great importance to the local economy [5]. The cultivated area in New Valley increased from about 18,000 hectares in 1988 to approximately 29,000 hectares in 1998 [6] due to land reclamation [7]; crop cultivation is the primary water-consuming sector in this area, consuming more than 75% of the water available in New Valley [5]. The increase in the

size of the cultivated areas in New Valley, therefore, poses a threat to the limited natural resources available in this region, especially water [8].

As one of the essential elements in the hydrological cycle in the Egyptian Western Desert, the Nubian Sandstone Aquifer System (NSAS) is a thick permeable sandstone formation located under the eastern end of the Sahara Desert, which extends across Egypt, Sudan, Chad, and Libya in northeastern Africa [9], occupying about 2×10^6 km².

As the primary groundwater-consuming sector in New Valley since the 1990s, agriculture was expanded through the exploitation of water resources from the NSAS in response to the expected future population growth. However, the large-scale development of oasis agriculture is expected to lower the groundwater table around the oases [10]. As one of the largest and most extensively investigated fossil water aquifer systems in the world, the average depletion rate across the NSAS in Egypt is estimated to have been -3.38 ± 0.21 mm/yr (-2.23 ± 0.14 km³/yr) from April 2002 to June 2016 [11].

A total of 98% of the available freshwater utilized for agricultural, industrial, or domestic activities in this region is supplied by NSAS's fossil water. However, the present water resource situation in the study area is quite bleak: about 30% of the land that was cultivated in 1965 is currently abandoned because of water shortages [5]. Unmanaged groundwater extraction in Egypt has led to several changes, as seen in the hydraulic head patterns and noticeable cones of depression that have appeared in the past 50 years [1]. Egyptian decision-makers face a challenge in providing and maintaining sustainable water resource management [11].

Accurate estimation of land use/land cover change (LULCC) is essential in order to obtain an improved understanding of its impacts on environmental systems and natural resources, enabling the provision of appropriate sustainable management practices. For this, an improved understanding of LULCC impacts on environmental systems and natural resources is necessary. While a few studies have shed light on the LULCCs of oases in New Valley [10,12–16], highlighting the space–time dynamics of oasis land use in New Valley, they are limited in terms of their geographic scope—i.e., they focus on the area of a single oasis comprising a few small districts. Nevertheless, the existing literature does not provide a detailed and comprehensive understanding of the pattern of LULCC across all of the oases in the entire New Valley. To overcome this research gap, the present study embarks on producing detailed, long-term LULC maps of the oases of the entire New Valley Governorate in Egypt in order to provide insights into the varying levels of interplay between humans and the physical environment in this region. At the same time, LULC can map the extent and distribution of agricultural areas to estimate the irrigation water volumes in irrigated areas. Estimating irrigation water consumption can not only help with determining irrigation water food production [17] but is also advantageous for the sustainability assessment of groundwater in arid regions such as the Western Desert of Egypt.

Furthermore, the quantification of water consumption is crucial in evaluating water sustainability projects and is of extreme importance to the current water policy. It is also one of the main goals of studies that use remote sensing observations for irrigation estimation [18]. Although several approaches for estimating water demand or water consumption have been tested and approved worldwide [19–21], these require accurate meteorological data, ideally measured in the field, even though in most parts of the world these are often unavailable. Moreover, it has been shown that crop coefficients are site-specific and should be determined locally, suggesting the need for dedicated experimental activities. Therefore, the accuracy of estimates decreases whenever farming or environmental factors cause limitations to crop growth and where local data on crop coefficients are missing. In particular, this inaccuracy can sometimes cause inconveniences when the method is used for irrigation management or scheduling [19].

For areas such as the oasis in Western Egypt, which is completely supported by groundwater, the use of water resources can also be quantified by the extraction of groundwater. The emergence of GRACE makes the quantification of groundwater resource consumption

possible. Before GRACE, the existing time and spatial resolution observation networks were not sufficient to fully characterize the water balance on the regional to continental scale. Since its launch, GRACE has come to be used in hydrological analyses and has been deemed one of the most potent tools in the remote sensing field. Based on recent advances, it provides excellent opportunities for understanding the large-scale changes in polar ice, soil moisture, surface water, and groundwater storage and has led to significant results being achieved in these fields [22–26]. Significantly, GRACE satellites have been proven to be exceedingly successful for detecting groundwater changes that could not previously be analyzed. GRACE data have been widely used to calculate aquifer recharge, depletion rates, and variability [27–47]. Nevertheless, it is difficult to confirm depleted water volumes with actual water use given the lack of field monitoring networks as well as recent global groundwater studies carried out over the study area.

Thus, the main purpose of the present study is to produce detailed, long-term LULC maps of the oases in order to identify the land cover changes through investigating the primary water consumption patterns to quantify the water consumption of the study area by two different approaches (LULC based on optical remote sensing data and groundwater storage changes based on GRACE (Gravity Recovery Climate Experiment) satellite data) and compare and contrast the quantitative results obtained using the two approaches.

This paper assumed that the Nubian Sandstone Aquifer in the New Valley could not be recharged by external sources; there is negligible rainfall in northern parts of the Nubian Sandstone Aquifer System [48,49]. The aquifer depletion could only be attributed to water extraction in the Nubian Sandstone Aquifer Systems. According to a wide array of age dating techniques, the water in the Nubian aquifers comes from several past pluvial episodes [50]. The last rainy season caused the recharge that occurred 8000 years ago [51]. Rainfall currently delivers minimal recharge water to the recharge area, northwest Sudan and Uwein at Upland, situated on the border of Egypt, Libya, and Sudan [52]. Mohamed et al. [48] indicated that the Dakhla subbasin and the northern Kufra section of the Nubian Sandstone Aquifer System receive negligible recharge due to the scarcity of precipitation in these areas. Meanwhile, no correlation has been found between the atmospheric hydrological fluxes and the GWS in the NSAS, as would be expected for a fossil aquifer [49]. Thus, the irrigation water in the Dakhla oasis is mostly fossil water with ancient roots [53].

For arid areas such as Egypt's oases, analyzing and clarifying the LULCCs and water usage are extremely important for formulating agricultural development, water resource utilization, and sustainability management plans.

2. Materials and Methods

2.1. Study Area

The New Valley Governorate or Wadi Gedid Governorate is located in the country's southwest, comprising approximately half of Egypt's area. This spacious governorate is the country's largest and most sparsely populated; moreover, it is one of the most significant subnational divisions in the African continent and the world. The New Valley Governorate is 440,098 km² in area. Its administrative center is located in the Kharga Oasis. It is named after the New Valley Project, which the Egyptian government launched in 1960 to expand agricultural land outside the "old valley" along the Nile River.

The New Valley includes the Dakhla Oasis (25.34N, 28.56E), Kharga Oasis (25.26N, 30.33E), and Farafra Oasis (27.06N, 27.97E), as well as East Oweinat (22.42N, 28.28E) in the southwest (Figure 1). The rate of the increase in population in New Valley reached its peak in 1996, with Kharga having the largest population. The Farafra depression is the second biggest oasis in western Egypt and the smallest in terms of population (Table 1). East Oweinat is an area of ongoing development in Egypt; the initial phase of the project resulted in about 11,300 hectares of barren desert land being converted to fertile land. C. A. Robinson et al. [54] suggested that the wells in the vicinity of East Oweinat contain

low-salinity water; this is the reason why the East Oweinat area was selected for large-scale water resource development.

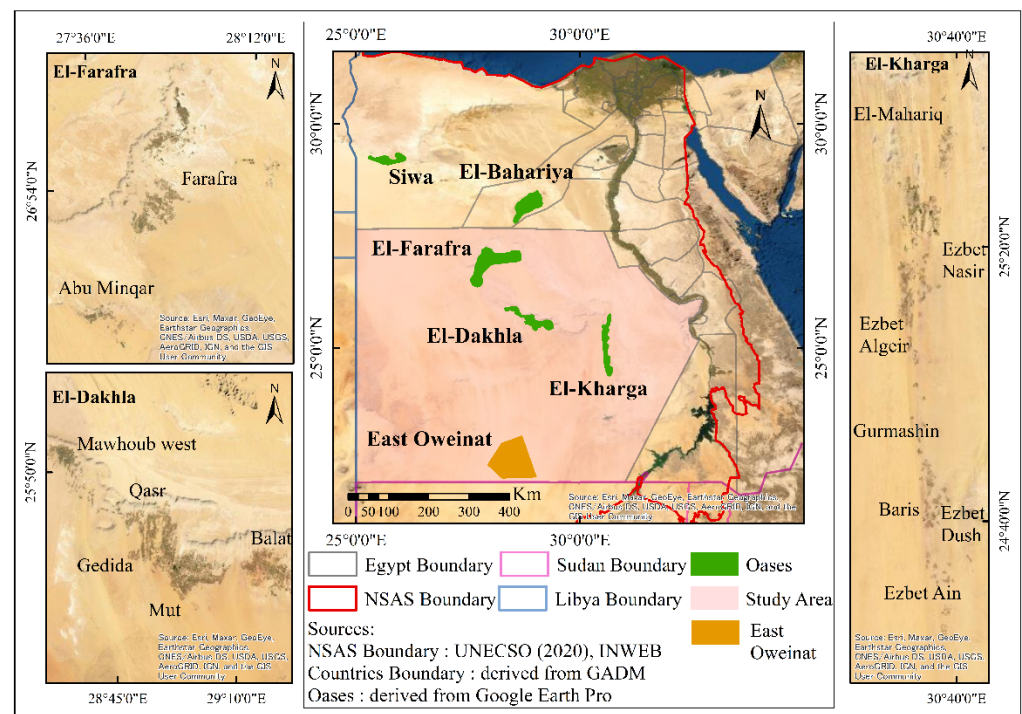


Figure 1. Location of the different oases in New Valley, Egypt.

Table 1. The population of the three oases in the New Valley Governorate (2017).

Oasis		Population		
		Urban	Rural	Total
Kharga	Kharga	71,936	18,078	90,014
	Baris	5568	7991	13,559
Dakhla	Balat	3457	8776	12,233
	Dakhla	23,216	66,405	89,621
Farafra	Farafra	6817	29,003	35,820

1. Note: Kharga and Dakhla Oases have been divided into two administrative districts (markaz) since 2006.
2. Source: CAPMAS, Final Results of Population, Housing, and Establishments (in Arabic), 2017, Table 1.

In New Valley, the annual rainfall is exceptionally scarce and insignificant (~1 mm/yr). The average annual ET_p of Dakhla Oasis from 2007 to 2016 was 1783 mm, while from May to August the monthly ET_p exceeded 200 mm [55]. There is a small rain-fed area in the study region. The irrigation water mainly comprises fossil water from the Nubian aquifer that originated in ancient times.

2.2. Dataset

2.2.1. Optical Remote Sensing Data

This study integrated the following different multispectral satellite images for LULCC analysis from 1986 to 2021 every three years: Landsat Thematic Mapper (TM), Operation Land Imager (OLI), and Sentinel-2 Level-2A surface reflectance (total of 68 images taken from 1986 to 2021 downloaded from the official USGS website).

2.2.2. Landsat 7 Collection 1 Tier 1 8-Day NDVI Composite

The agricultural area of New Valley for each oasis was extracted using Landsat 7 Collection 1 Tier 1 8-Day NDVI Composite data from 2002 to 2021. Landsat 7 Collection

1 Tier 1 composites are created using computed top-of-atmosphere (TOA) reflectance [56] from Tier 1 orthorectified scenes. The Normalized Difference Vegetation Index (NDVI) of Landsat 7 Collection 1 Tier 1 composites was calculated as $(\text{NIR} - \text{Red})/(\text{NIR} + \text{Red})$ [57] from the near-IR and red bands of each scene and ranged from -1.0 to 1.0 . The Landsat 7 Collection 1 Tier 1 composites were created from all of the scenes for each eight-day period beginning on 1 January and ending on 31 December. The final composite of the year, beginning on day 361, would, therefore, be three days later than the first composite of the following year.

2.2.3. GRACE and GRACE-FO Mascon Data

The GRACE (Gravity Recovery and Climate Experiment) mission, launched on 17 March 2002 [58], maps the Earth's gravitational field by accurately measuring the distance between two identical space crafts [59] in a polar orbit that is approximately 220 km (137 miles) apart and 500 km (310 miles) above the Earth and has a K-band microwave range and speed measurement system that means that the measurement accuracy of the rate change between the two satellites is expected to be better than 1.0×10^{-6} m/s [60].

The GRACE mission was terminated in 2017. GRACE Follow-On (GRACE-FO) [61,62] began to take measurements in May 2018, continuing to the present. It tests the laser ranging interferometer (LRI), a new instrument used for inter-satellite ranging, in addition to the microwave K-band ranging system (KBR) previously used on GRACE satellites. GRACE satellites track spatiotemporal variations in water mass globally. Variations in water mass or storage are generally expressed as their equivalent, Equivalent Water Height (EWH).

In this study, two mascon solutions of GRACE from the Jet Propulsion Laboratory (JPL) and Center for Space Research (CSR) are operated owing to the fact that mascon solutions generally show lower levels of uncertainty compared to most SH solutions [63]. However, mascon solutions should only be utilized for basin-level time-series analyses at dimensions broader than 200,000 km².

The CSR mascon solutions (Release 06; version 02; $0.25^\circ \times 0.25^\circ$ grid; available at: <http://www2.csr.utexas.edu/grace/> (accessed on 4 October 2021)) approach applies the geodesic grid technique to model the surface of the Earth using an equal area grid [64,65]. In order to accurately reflect the coastlines defined in the RL06 mascon grid, the data are represented on a $\frac{1}{4}$ degree lon-lat grid. They also represent an equal-area geodesic grid of size $1^\circ \times 1^\circ$ at the equator, which is the current native resolution of CSR RL06 mascon solutions.

The JPL mascon solutions (Release 06; version 02; $0.5^\circ \times 0.5^\circ$ grid; available at: <https://podaac-tools.jpl.nasa.gov/> (accessed on 4 October 2021)) provide monthly gravity field variations for 4551 equal areas of 3° spherical caps. This study relied on coastal resolution improvement (CRI)-filtered data (the CRI-filtered version of the mascon solution [62,66–68]), in which the coastlines are well-defined.

2.2.4. Other

Natural and agricultural statistical datasets were used to quantify the balance between water consumption and groundwater extraction. According to the Egyptian Statistical Yearbook from 2002 to 2020 [2,3,69,70] (Table 2), the population, total cropping area, and quantity of irrigation water used for the three agricultural seasons of Egypt were used. Furthermore, Google Earth was referenced to collect sample points and classify the accuracy of the LULC maps. Table 2 summarizes the characteristics of these datasets.

2.3. Methodology

The main framework of this study is shown in Figure 2. The LULC maps of three cases from 1986 to 2021 every three years in New Valley were constructed using optical remote sensing data in order to better understand the pattern of LULCC across the three main oases in the New Valley. The agricultural area data for each year from 2002 to 2021 were extracted based on the average results of the Landsat 7 Collection 1 Tier 1 8-Day

NDVI Composite data from the late part of the growing season (January to March) and then combined with the threshold method (threshold 0.3 [55]). The groundwater storage changes from 2002 to 2021 in New Valley were quantified using the GRACE CSR and JPL mascon solutions. The statistical (e.g., Yearbook) data were used to quantify the irrigation water per unit value, which was combined with the agricultural area to calculate the total irrigation water use of New Valley (Figure 2).

Table 2. Datasets used in this study.

Dataset Category	Study Area	Sensor	Date	Resolution	Path/Row	Source		
Remote sensing data	Dakhla Oasis	Landsat TM	1986 ~ 2011	30 m	P177/R42	USGS		
		Landsat OLI	2014 ~ 2019					
		Sentinel-2	2021					
	Kharga Oasis	Landsat TM	1987 ~ 2011	30 m	P176/R42-P176/R43			
		Landsat OLI	2014 ~ 2019					
		Sentinel-2	2021					
	Farafra Oasis	Landsat TM	1987 ~ 2011	30 m	P178/R41-P178/R42			
		Landsat OLI	2014 ~ 2019					
		Sentinel-2	2021					
	Three oases and East Oweinat	Landsat 7 Collection 1 Tier 1 8-Day NDVI Composite	2002~2021	30 m	Three oases and East Oweinat		Google Earth Engine Platform	
	GRACE	New Valley	GRACE	2002~2021	0.25°/0.5°		-	CSR/JPL
	Statistical data	Egyptian Statistical Yearbook [2,3,69,70]						
Reference data	Google Earth Pro				P176/R42-P178/R42			

2.3.1. Land Cover Mapping Pre-Processing

All Landsat images used for LULC classification were geometrically corrected using the ENVI software. The reference system used was the UTM map projection Zone 35 North (Dakhla Oasis and Farafra Oasis) and Zone 36 North (Kharga Oasis) from the WGS 1984 datum. Sentinel-2 Level-2A provided orthorectified atmospherically corrected surface reflectance data. Clouds seldom obscure satellite images taken in the Western Desert of Egypt [55]. The chosen dates for each image fell in the late part of the growing season.

LUC Classification Method

This study used the object-based image analysis (OBIA) method [71,72] to map LULC according to shape, landscape, and personal experiences. OBIA, which is a combination

of multiresolution image segmentation [73] and the nearest neighbor (NN) classification method [74], was used to identify LULCCs. Research shows that the combination of segmentation into image objects, use of the NN classifier, and integration of expert knowledge yields a substantially improved classification accuracy for a scene, compared to a per-pixel method [75].

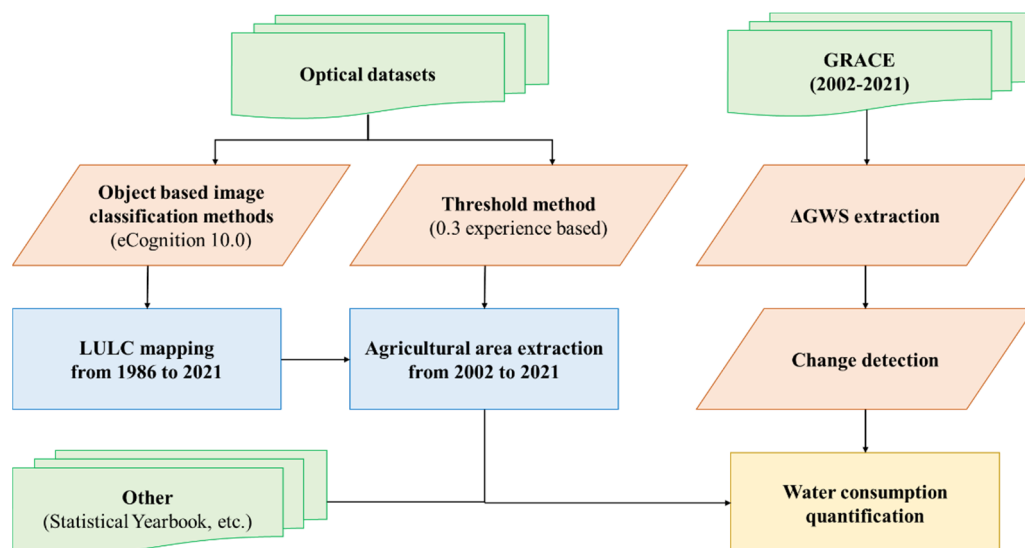


Figure 2. Research framework. Green indicates the datasets used, orange indicates methods, blue indicates staged results, and yellow final objectives.

OBIA is implemented in the software “eCognition” [76], and the final feature extraction and classification are, therefore, highly dependent on the quality of segmentation [77]. It has provided a new bridge for the spatial concepts applied in multiscale landscape analysis and more possibilities for geographic information systems, geographic information science, and multiscale landscape analyses [78–84].

The classification of target categories was mainly carried out based on spectral features, geometric features, and custom features. The possible land cover types were divided into four categories: urban area, surface water body, agricultural land, and desert (Table 3). The scale parameter was set at 5 [85] for all LC classes, because all types of land in the study area were in small units and spread out. The color and shape parameters were adjusted to 0.9 and 0.1, respectively [86]. All of the collected images were dated from the late part of the growing season (January to March); thus, any trends related to seasonal differences were not taken into consideration.

Table 3. Land use land cover classification system.

Level 1	Level 2	Definition
Agricultural land	-	Area cultivated for crops
Water body	-	Includes lake-covered land, agricultural drainage, and artificial water tanks
Urban	Man-made	Human inhabited areas such as cities and countryside
	Bare land	Land with spectral characteristics close to fallow farmland, abandoned cultivated land, and residential areas
Desert	-	Barren areas with completely sandy ground, little vegetation, low levels of rain, dry air

2.3.2. Water Usage Quantification

After revealing the changes in LULC, we attempted to quantify the primary water consumption pattern (i.e., irrigation for agricultural use) in order to estimate the effect of LULC on the water consumption of oases in the study area. The irrigation water per unit value was calculated based on the irrigation water used in the three agricultural seasons of Egypt (from 2002 to 2019); the total cropping area of Egypt (from 2002 to 2019) [$W_{\text{Egypt}}/A_{\text{Egypt}}$] was determined from the Egypt Statistical Yearbook (Table 2).

The Landsat 7 Collection 1 Tier 1 8-Day NDVI Composite was adopted to extract the total available cultivated land in the area of New Valley (Dakhla, Kharga, Farafra, and East Oweinat) from 2002 to 2021 using a threshold of 0.3 [55]. The average irrigation water use per unit from 2002 to 2019 was used to quantify the irrigation water consumption in 2020 and 2021. In the agricultural area, the changes in agricultural irrigation water consumption (per year) from 2002 to 2021 were determined.

Using the agricultural land area identified from the Landsat 7 Collection 1 Tier 1 8-Day NDVI Composite [$A_{\text{New Valley Oases}}$], the overall irrigation water consumption from 2002 to 2021 was calculated (Equation (1)).

$$W_{\text{New Valley Oases}} = (W_{\text{Egypt}}/A_{\text{Egypt}}) \times A_{\text{New Valley Oases}} \quad (1)$$

Here, $W_{\text{New-Valley oases}}$ is the irrigation water of the oases in the New Valley Governorate; W_{Egypt} represents the quantity of irrigation water used for the three agricultural seasons of Egypt (from 2002 to 2019); A_{Egypt} represents the total cropping area of Egypt (from 2002 to 2019); $A_{\text{New Valley oases}}$ represents the agricultural area of the oases in New Valley Governorate. Domestic water usage from 2002 to 2021 was estimated by applying population data.

2.3.3. Extraction of Groundwater Storage Changes

Groundwater storage changes from GRACE were computed from terrestrial water storage changes (ΔTWS) in other terrestrial water stores, including soil moisture storage (ΔSMS), surface water storage (ΔSWS), and snow water storage (ΔSNS) [27], utilizing data from land surface models (LSMs) either exclusively [87–90] or in combination with in situ observations [46,91].

Frappart [27] described several methods that could be applied to solve a wide range of hydro-climatic conditions; these included the use of in situ records, model outputs, and remotely sensed observations. He indicated that, in the most straightforward cases where surface water is negligible and snow is non-existent, the groundwater storage changes (ΔGWS) in arid and semi-arid areas can be calculated. The equation used for extracting the changes in groundwater storage (ΔGWS) in the study area is:

$$\Delta\text{GWS} = \Delta\text{TWS} - \Delta\text{SMS}, \quad (2)$$

The soil moisture in hyper-arid areas is generally very low [92]; therefore, the effects of ΔSMS in the study area were not considered. The equation can be simplified to:

$$\Delta\text{GWS} = \Delta\text{TWS}, \quad (3)$$

where ΔGWS , ΔSWS , and ΔSMS represent the change in groundwater, surface water, and soil moisture storage, respectively, with respect to the temporal period mean.

The secular trend in groundwater storage changes was extracted from the GRACE data by simultaneously fitting the trend of each GWS time series. The standard deviation of the extracted time series was interpreted as the trend error for ΔGWS . The generated trend data were then statistically analyzed using change-point detection to identify trends.

Mask across New Valley's area was applied to the two types of GRACE mascon solution. These GRACE mascon solutions were averaged over New Valley's area. The arithmetic mean of the two mascon solutions was applied to extract the groundwater

consumption by multiplying the New Valley's area, as the average was found to reduce the noise in the gravity field solutions within the available scatter of the solutions [93]. Change point was analyzed on the Δ GWS time series.

3. Results

This paper mainly focused on the New Valley oases' land surface characteristics and water usage quantification. Object-based image analysis was applied to investigate changes in land use classes. We produced land cover maps for three oases in New Valley. The land cover classes identified in the study area were desert, water, urban land, and agricultural land (Table 3). The domestic water use during the period of population growth and the irrigation water usage during the period of changes in the cultivated area were quantified. The level of groundwater depletion that took place over 19 years was extracted. Further details about each type of land cover in the study area will be presented in the following sections.

3.1. LULC Classification Accuracy Assessment

Thirteen periods were selected for each oasis, as shown in Table 4. The accuracy of LULC mapping was evaluated by stratified random sampling. The number of reference points for each category was adjusted according to the area of the category. The original Landsat and Google Earth images were used as reference sources to classify reference points, and the overall accuracy and Kappa coefficient were calculated (Table 4).

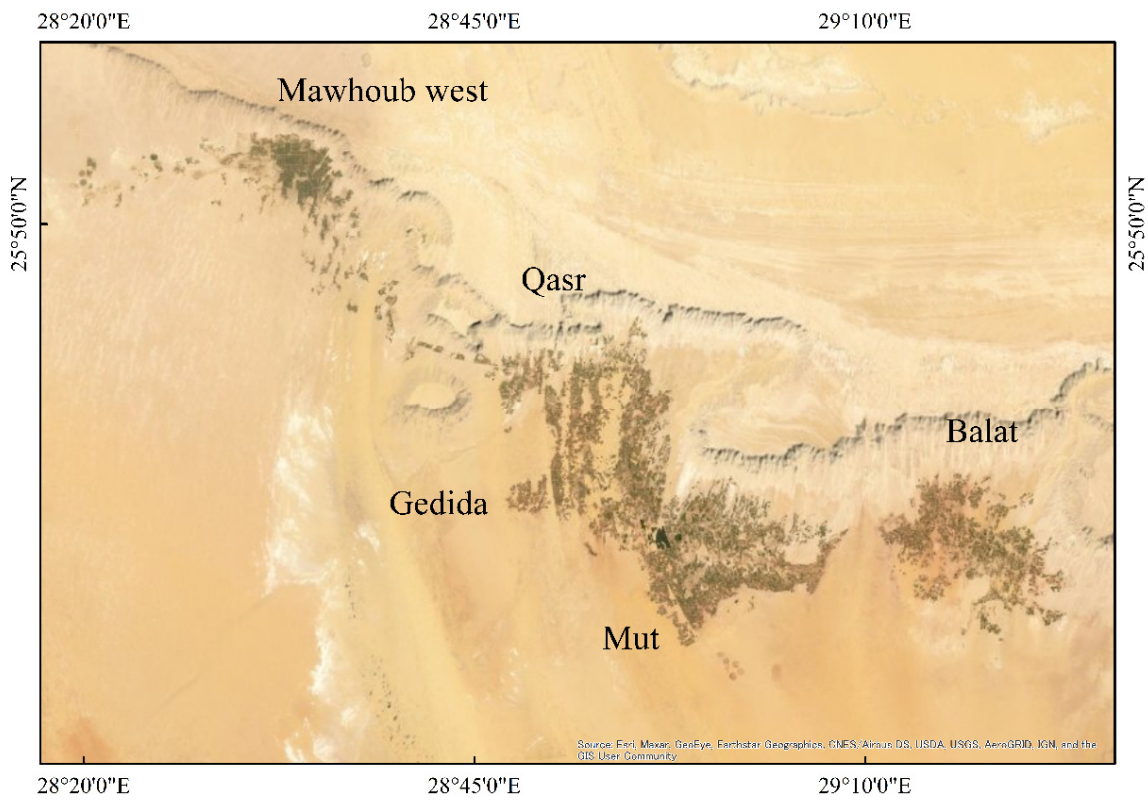
Table 4. LULC classification accuracy from 1986 to 2021.

Dakhla	Kappa Coefficient	Overall Accuracy (%)	Kharga	Kappa Coefficient	Overall Accuracy (%)	Farafra	Kappa Coefficient	Overall Accuracy (%)
1986/03	0.93	95	1987/02	0.96	97	1987/01	0.95	97
1989/03	0.92	95	1990/03	0.93	96	1990/03	0.87	94
1992/03	0.94	96	1993/03	0.91	94	1993/03	0.91	95
1996/03	0.92	95	1996/02	0.97	98	1996/03	0.94	97
1999/03	0.87	92	1999/03	0.97	98	1999/03	0.93	96
2002/03	0.86	89	2002/01	0.94	97	2002/01	0.92	95
2005/03	0.84	88	2005/03	0.95	97	2005/03	0.90	93
2008/03	0.80	86	2008/03	0.95	97	2009/03	0.93	95
2011/03	0.81	87	2011/03	0.97	98	2011/03	0.93	96
2014/03	0.78	84	2014/03	0.97	98	2014/02	0.95	97
2017/03	0.91	94	2017/03	0.98	99	2017/03	0.93	96
2019/03	0.94	95	2019/02	0.96	98	2019/03	0.94	96
2021/03	0.86	91	2021/03	0.97	98	2021/03	0.94	96

Table 4 presents the error matrix and accuracy assessment for the classification image of each oasis. The sampling points across the study area were taken randomly and were found to be relatively uniformly distributed among the types of LULC. The OBIA method was able to identify the LULC types successfully and with a relatively high accuracy.

3.2. LULC Classification Results of the Three Oases in New Valley

The 30 m resolution land cover map from 2002 to 2019 and the 10 m resolution land cover map for 2021 were created using the OBIA method, which involved sorting the classes into urban area, agricultural land, desert, and water bodies, as shown in Table 3 and Figures 3–5. Bare land samples could not be filtered out by the sampling method applied because of the similarity between the spectra of bare land and urban area. Accordingly, bare land was not shown independently in the classification results.



(i)

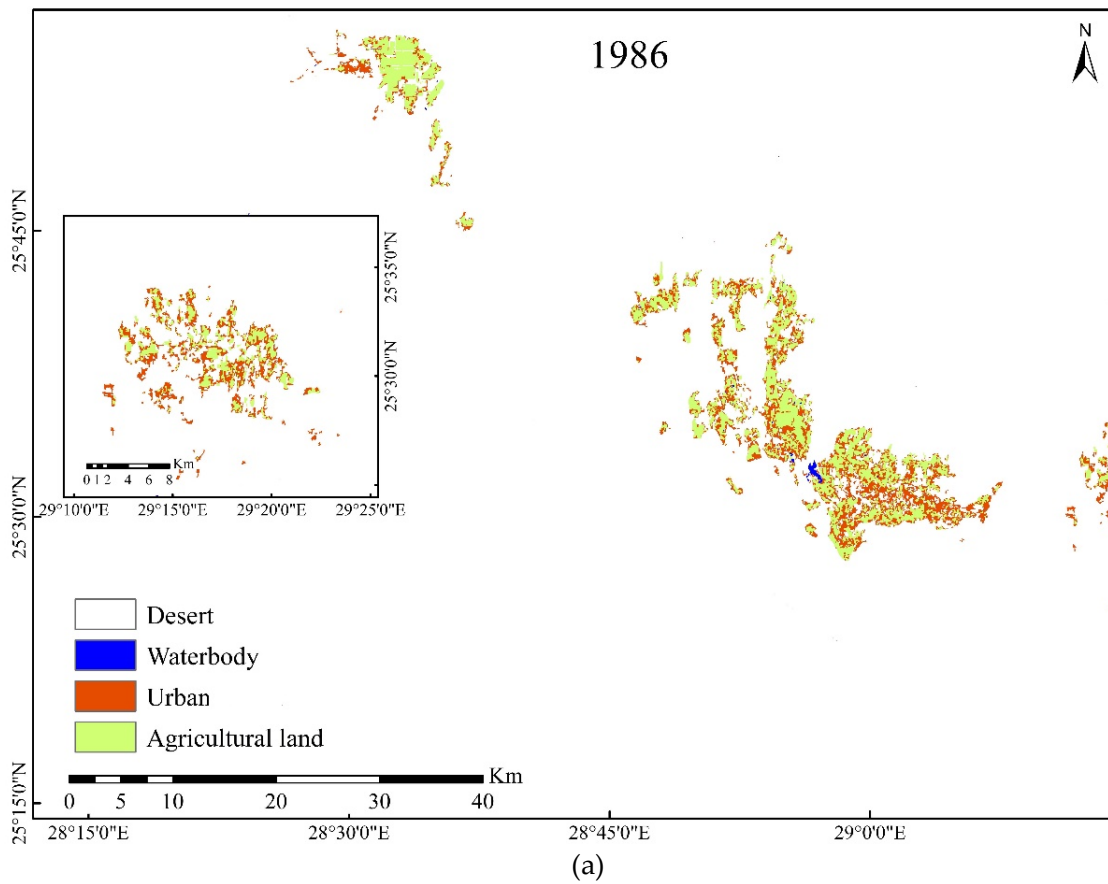
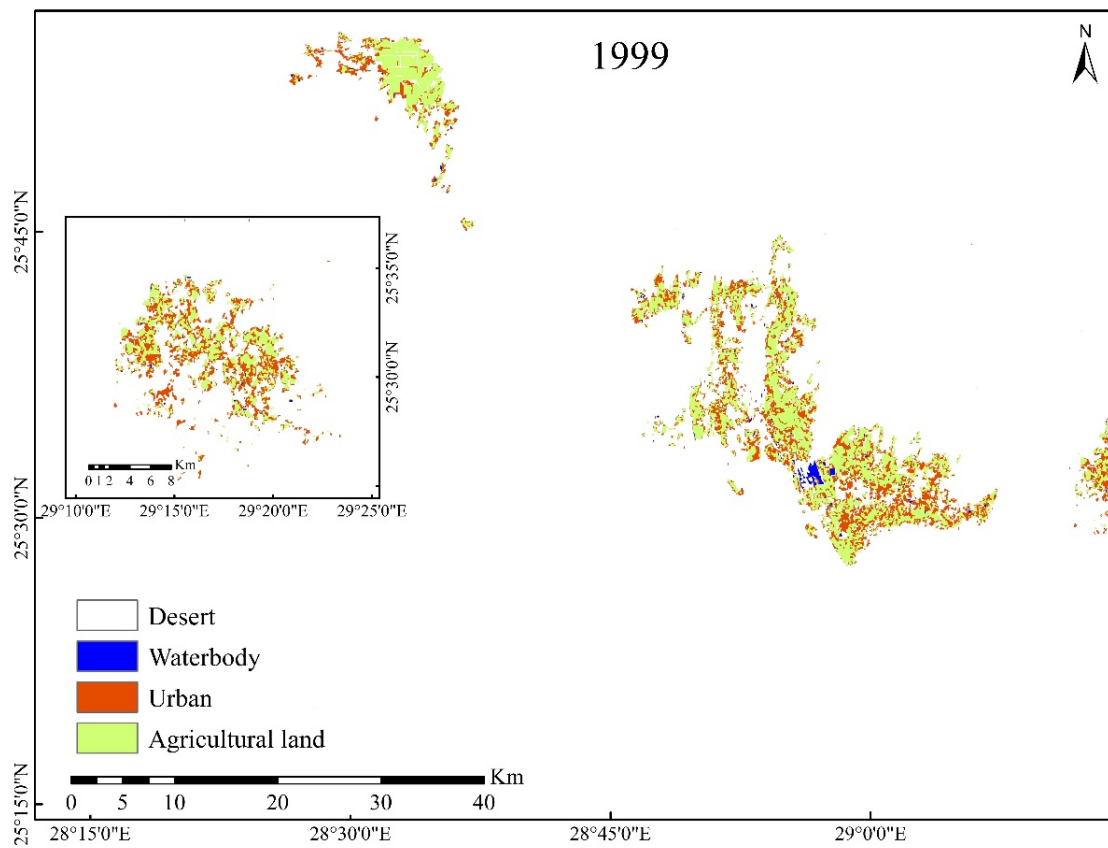
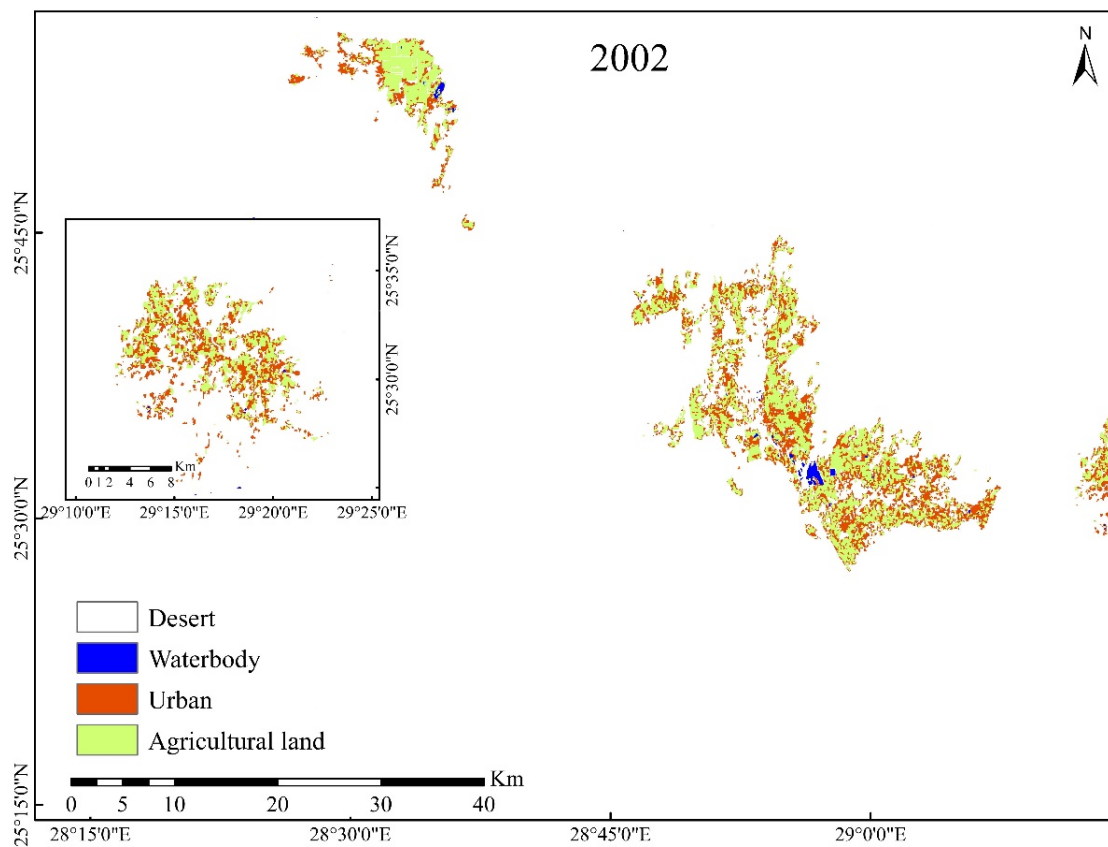


Figure 3. Cont.

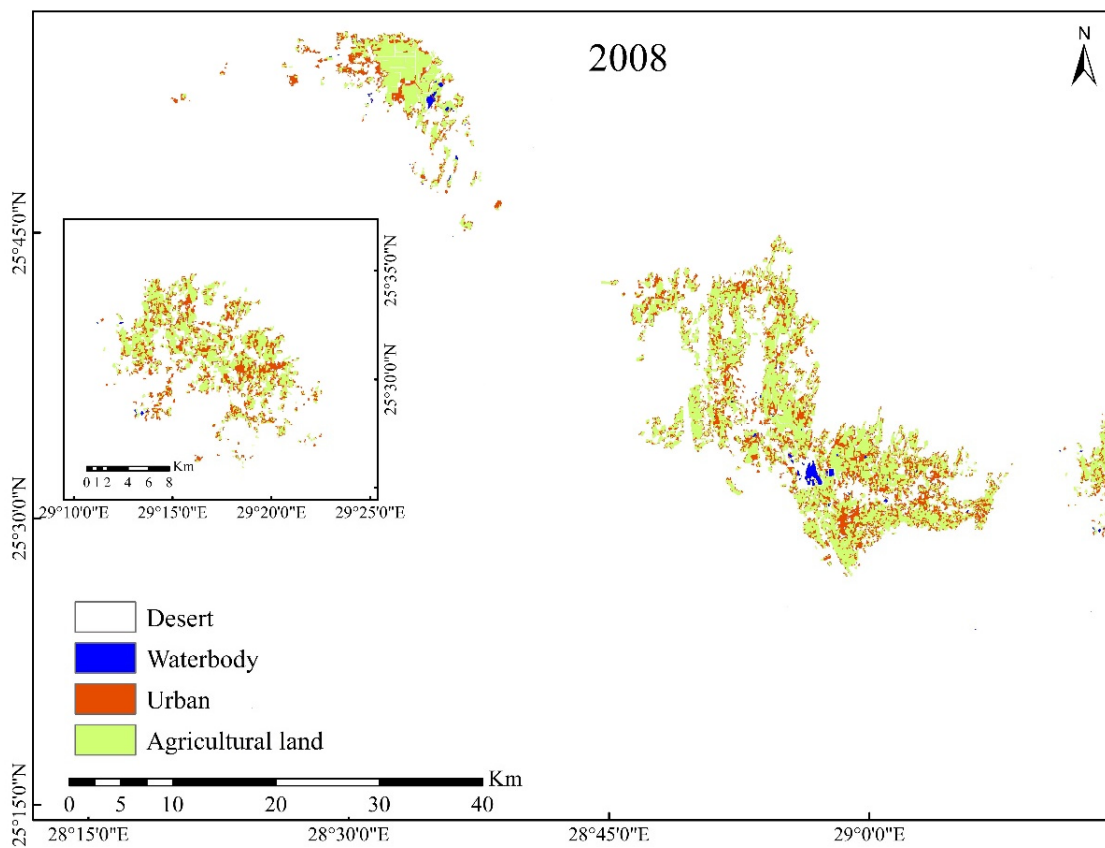


(b)

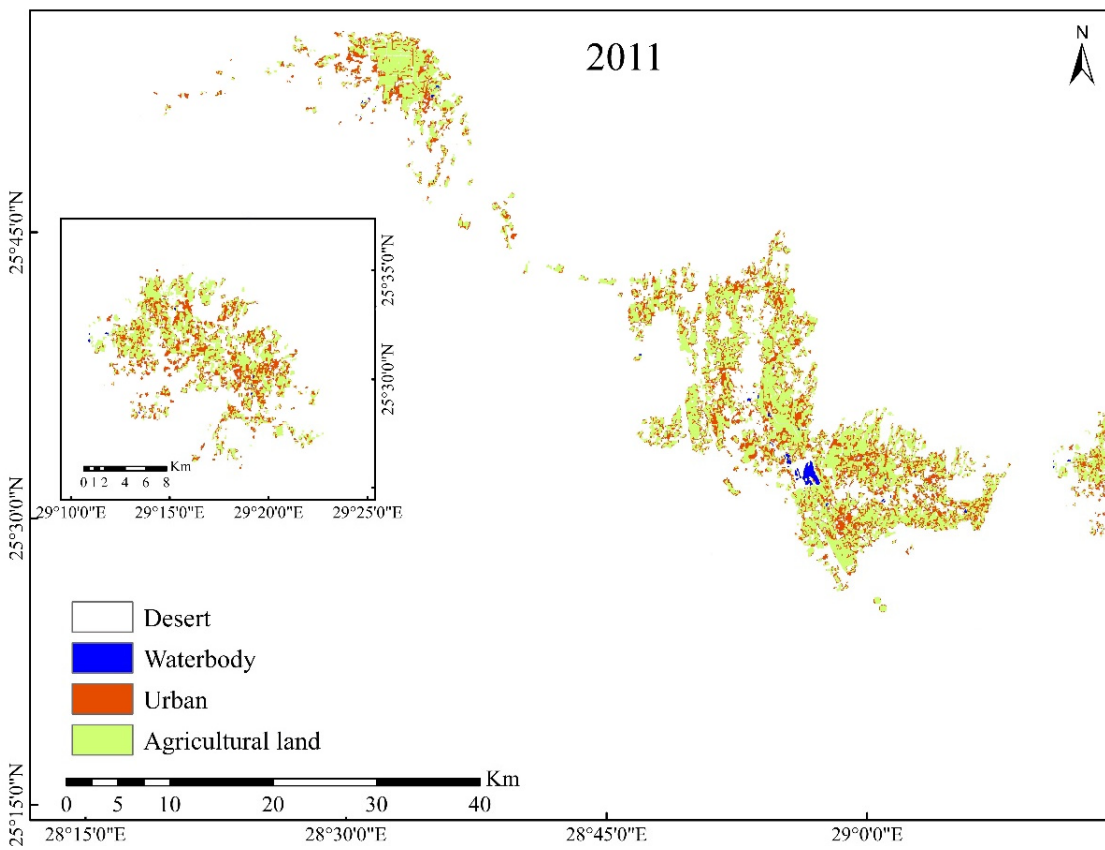


(c)

Figure 3. Cont.



(d)



(e)

Figure 3. Cont.

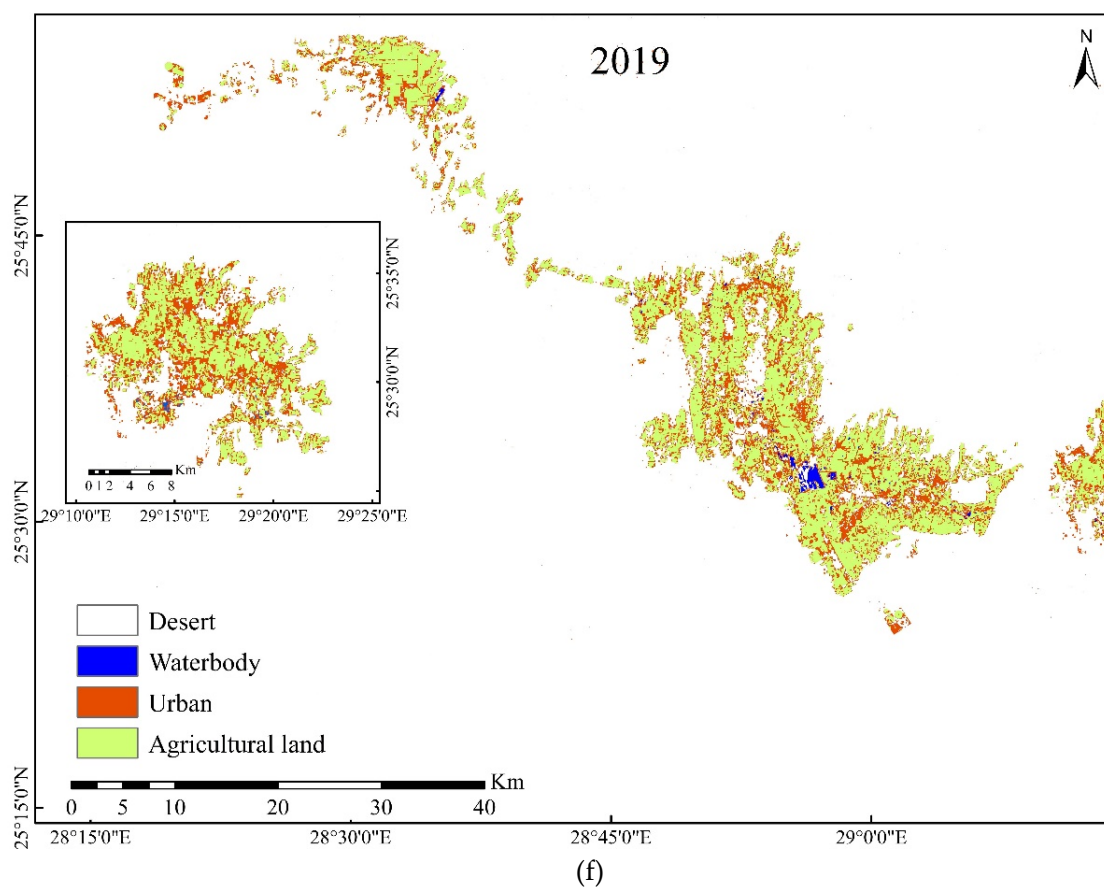


Figure 3. Land use and land cover classification maps of Dakhla Oasis; (i) distribution of regions in Dakhla Oasis, (a) 1986, (b) 1999, (c) 2002, (d) 2008, (e) 2011, and (f) 2019; refer to Supplementary Figure S1 for all maps from 1986 to 2021.

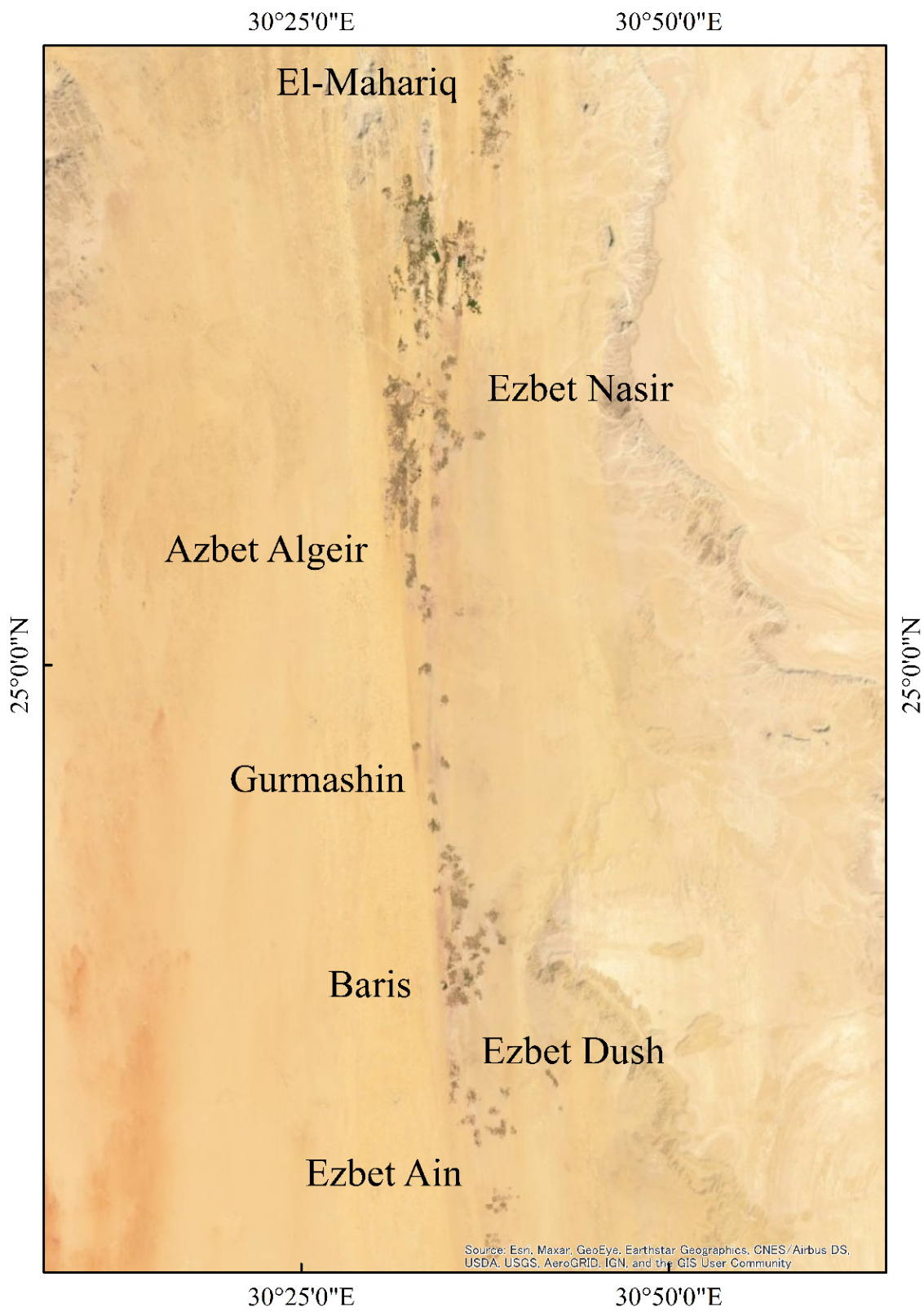
LULC maps of the three oases in New Valley were established every three years. We summarize the six periods with apparent changes over the 35 years in each oasis in Figures 3–5, and the remaining images are shown in the Supplementary Materials.

3.2.1. Dakhla Oasis

The LULC distribution of Dakhla Oasis consisted of three separate areas—namely, Mawhoub West in the northwest; Qasr, Gedida, and Mut in the southeast; and Balat in the east (Figure 3i).

The Mawhoub West area has been expanding outwards continuously since 1986 (Figure 3a–c) and has extended to the west and southeast since 2008 (Figure 3d). From 2008 to 2011, there was an eastward chain-like expansion from Mawhoub West (Figure 3e). After 2011, this chain-like expansion became more pronounced (Figure 3e–f). At the same time, Mawhoub West extended westward, expanding the entire area of Dakhla Oasis (Figure 3a–f). Since 2011, a small area of the center pivot has begun to appear in the lower southeastern part of the Dakhla Oasis; this expanded in 2017 (Figure 3e–f). The area consisting of Qasr, Gedida, and Mut in the southeast showed a trend of expanding outwards from 1986 to 2021 (Figures 3a–f and S1). The Balat area in the east first showed a fragmented distribution; by 2019, it had developed into a compact area (Figures 3a–f and S1).

During the development process of LULC in the whole region, agricultural land has changed the most. The changes in urban area closely follow the changes in agricultural land, and its growth generally relates to that of agricultural land.



(i)

Figure 4. Cont.

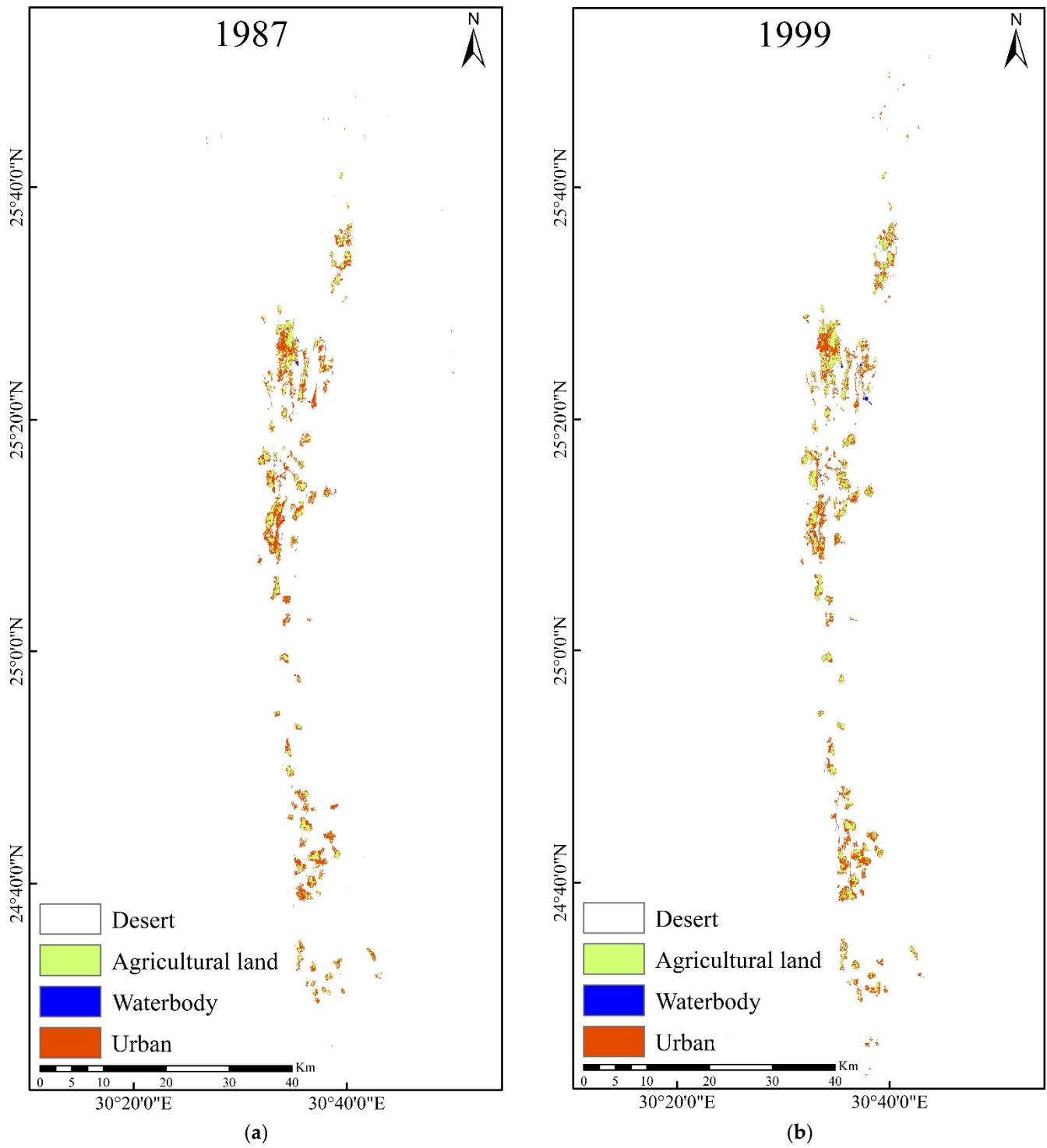


Figure 4. Cont.

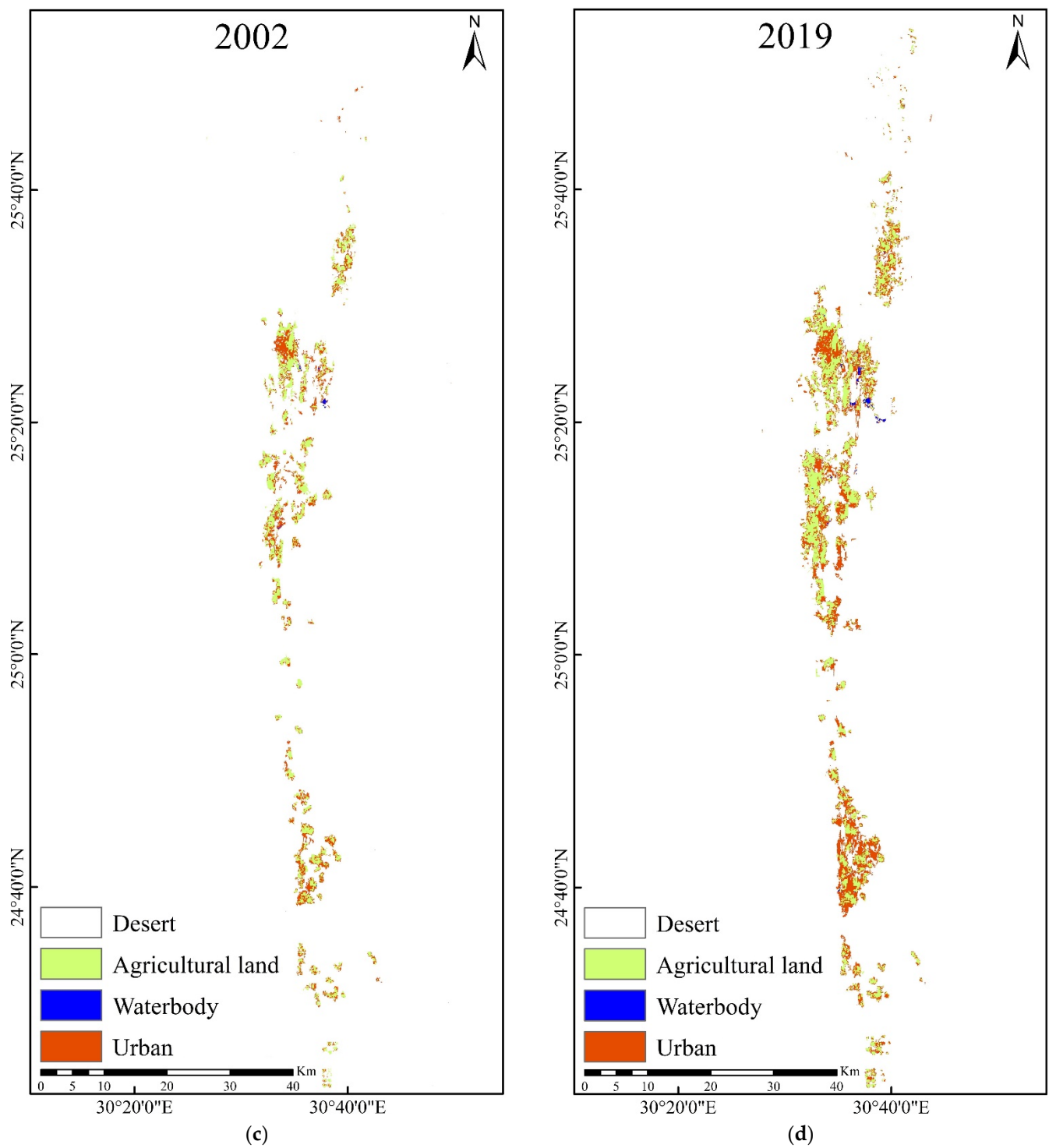
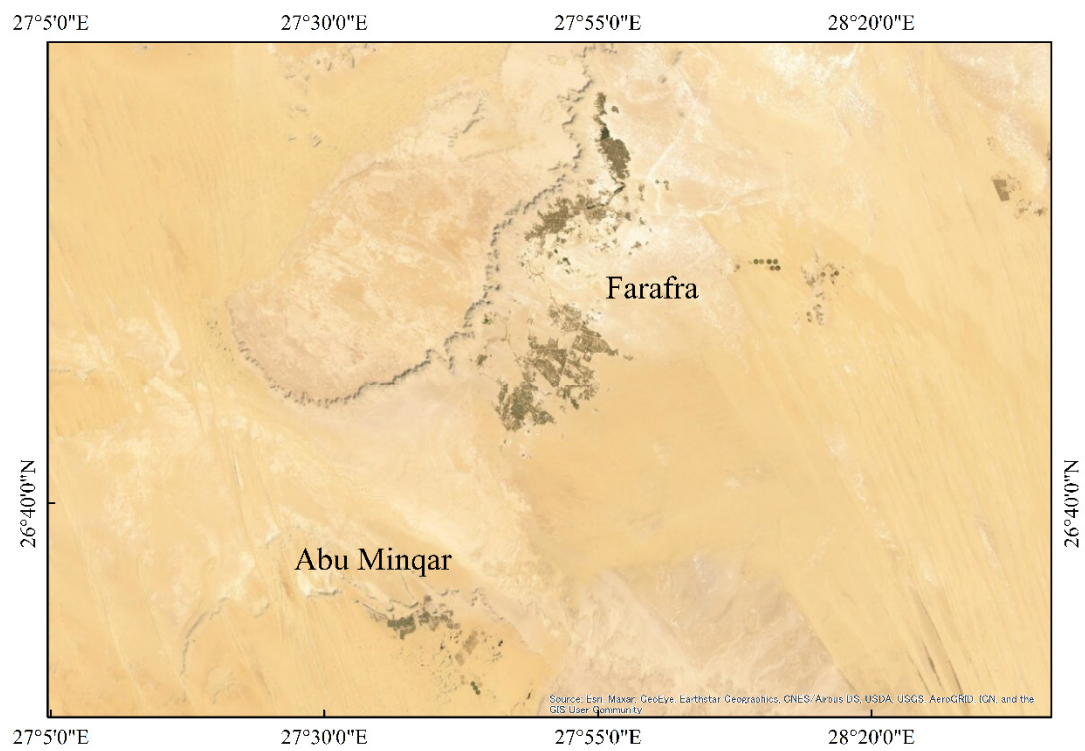
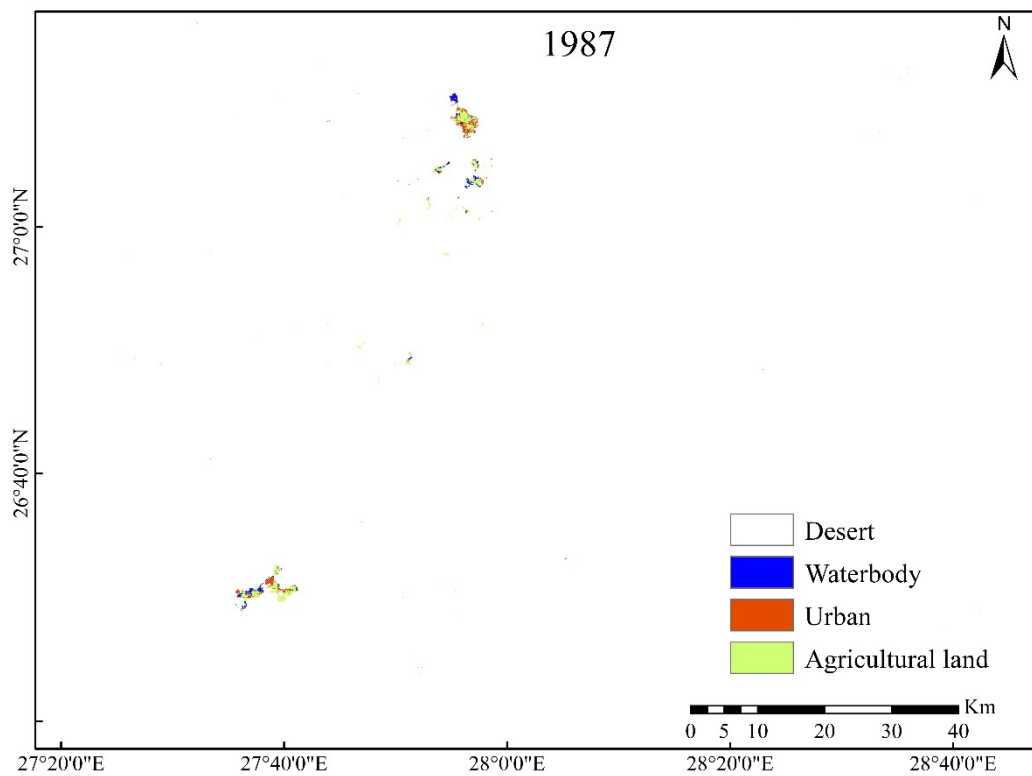


Figure 4. Land use and land cover classification maps of Kharga oasis; (i) distribution of regions in Kharga Oasis, (a) 1987, (b) 1999, (c) 2002, and (d) 2019; refer to Supplementary Figure S2 for all maps from 1987 to 2021.



(i)



(a)

Figure 5. Cont.

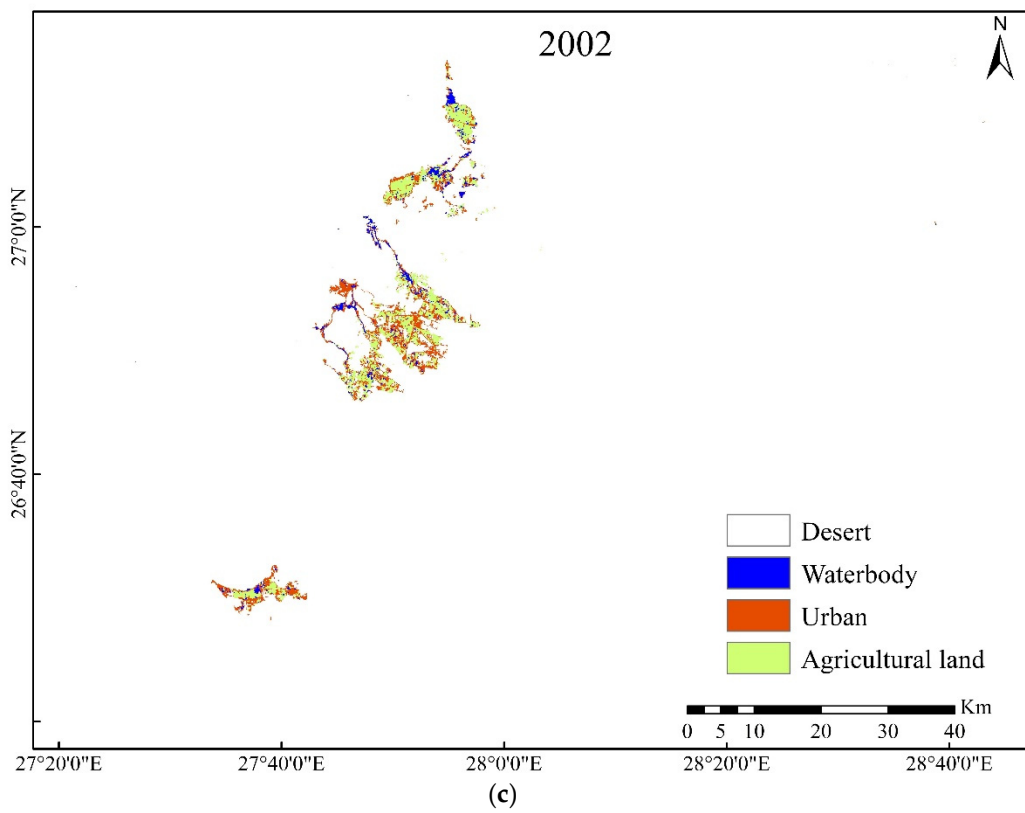
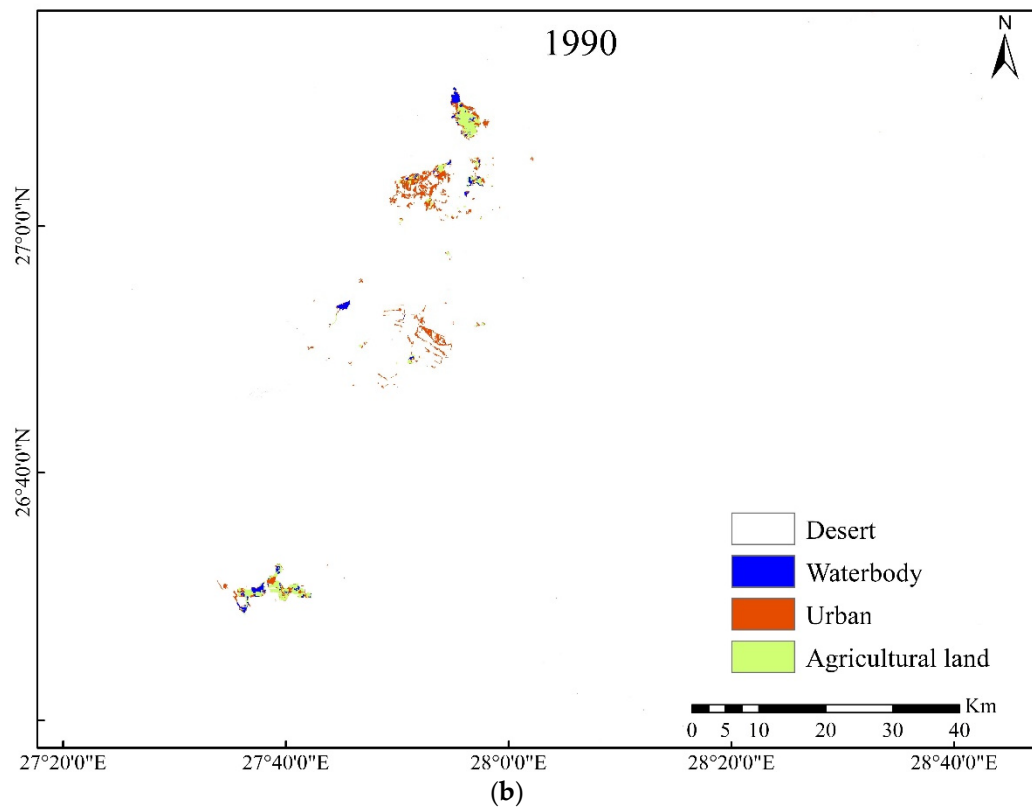


Figure 5. Cont.

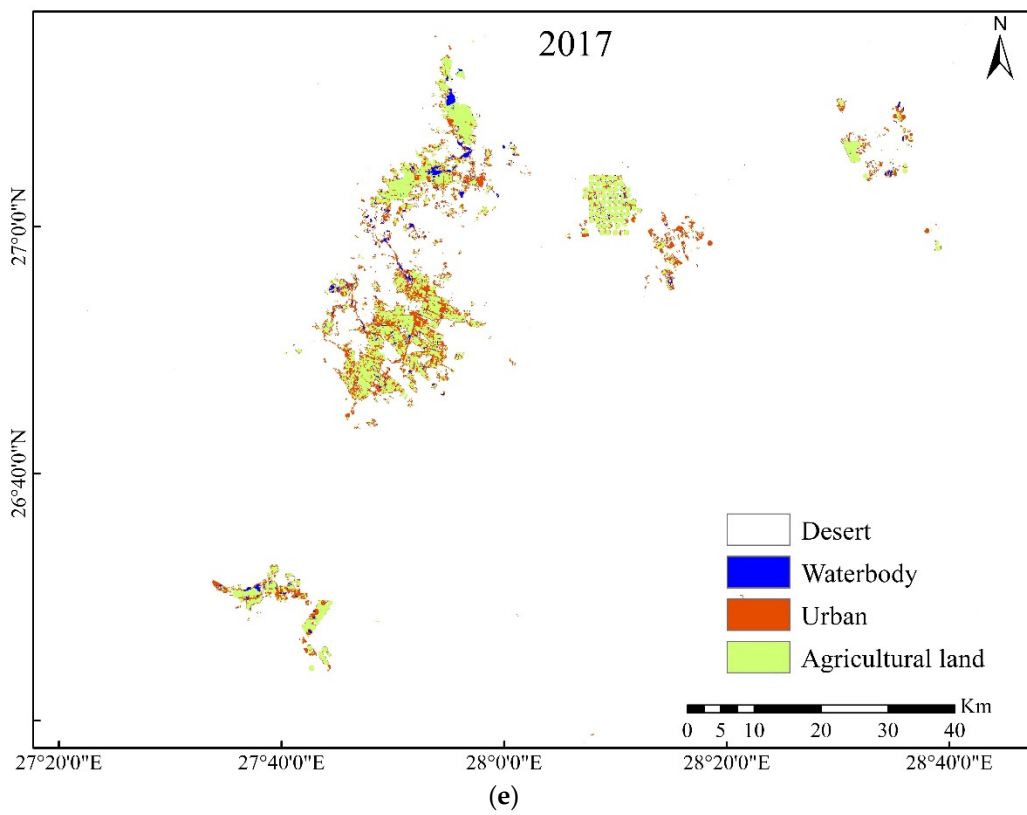
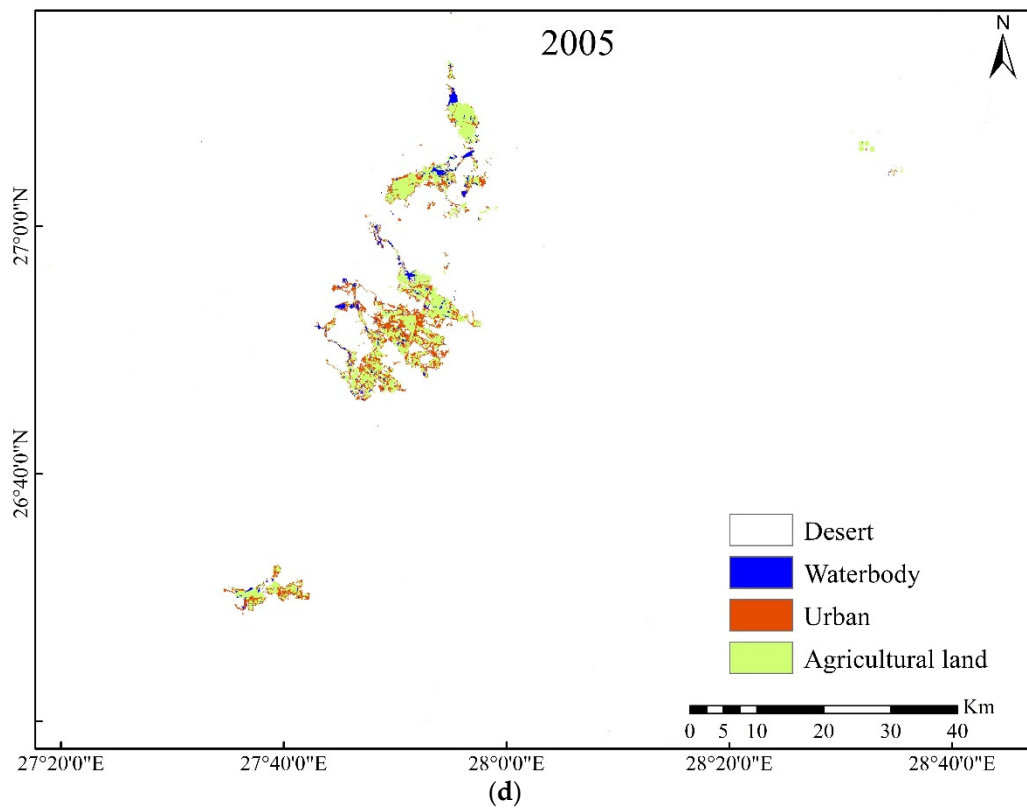


Figure 5. Cont.

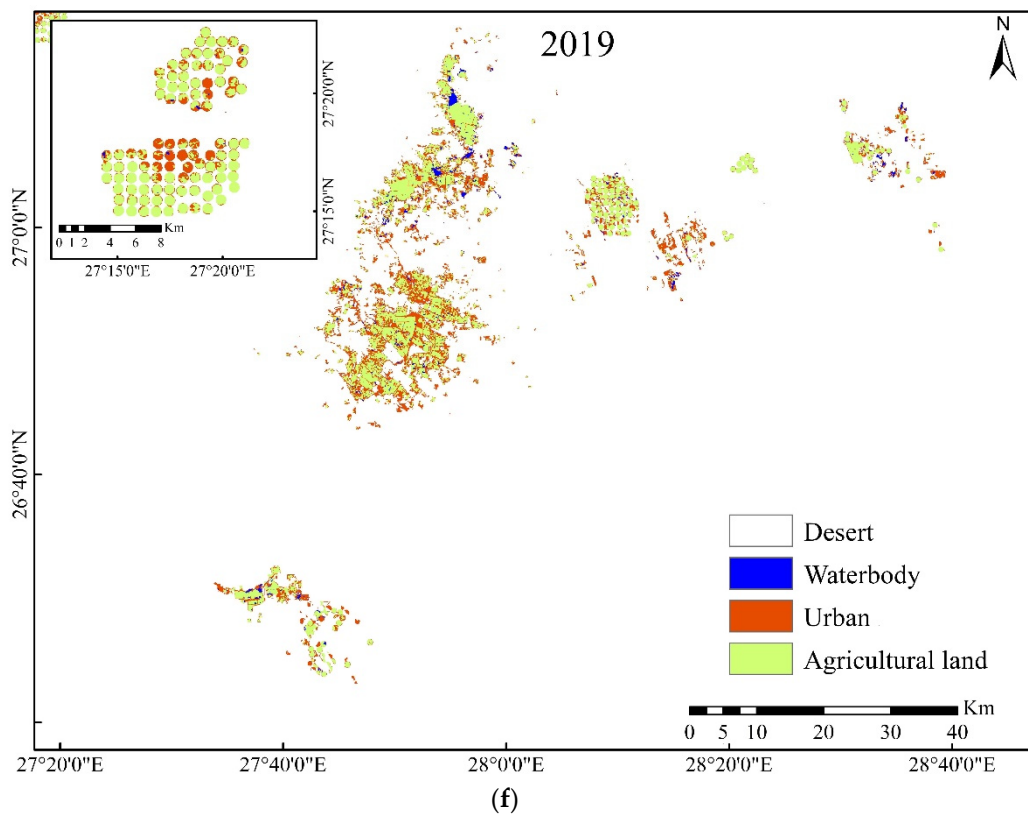


Figure 5. Land use and land cover classification maps of Farafra Oasis; (i) distribution of regions in Farafra Oasis, (a) 1987, (b) 1990, (c) 2002, (d) 2005, (e) 2017, and (f) 2019; refer to Supplementary Figure S3 for all maps from 1987 to 2021.

Figure 6a shows the changes in LULC types in Dakhla Oasis. The observation of changes over the entire study area demonstrated that changes in agricultural land, urban land, and water bodies were all apparent over a period of 35 years. Each class showed an overall trend of growth from 1986 to 2021 (Figure S1). The overall trends in the agricultural land changes (increase) in Dakhla Oasis were the same as those in urban area changes. However, in the short term, opposite trends in agricultural land and urban area changes were seen (Figure 6a), since the definition of urban area zoning includes both human-made non-agricultural land and fallow and abandoned cultivated lands (Table 3). Spectral characteristics show the fallow and abandoned agricultural lands as urban areas. Therefore, the periodic downward trends in the area of agricultural land are likely a reflection of changes in the agricultural land use (i.e., unused or in preparation) rather than an actual decrease in their area.

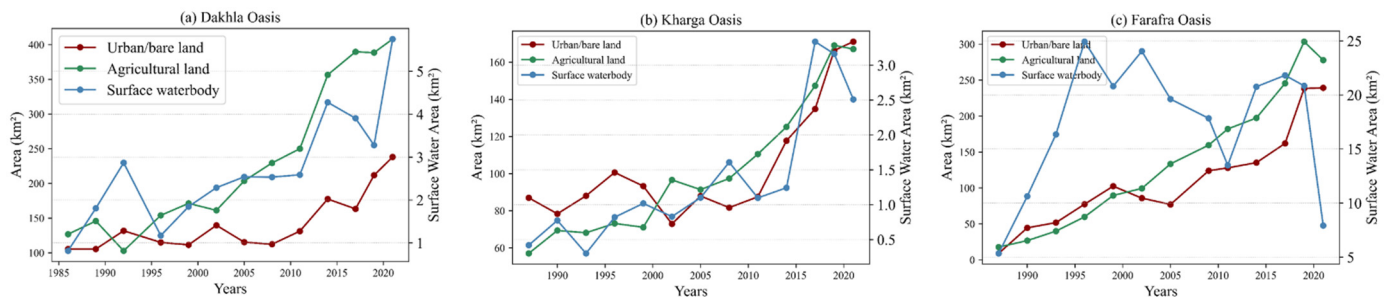


Figure 6. LULC development of the main classes of the three oases in New Valley from 1986 to 2021: (a) LULC development of main classes in Dakhla Oasis from 1986 to 2021; (b) LULC development of main classes in Kharga Oasis from 1987 to 2021; (c) LULC development of main classes in Farafra Oasis from 1986 to 2021.

The surface water body area in Dakhla Oasis revealed a marked trend of increase from 1986 to 1993 (Figure 6a). Except for the sharp trend of decrease demonstrated in the periods 1993–1996 and 2014–2019, the other changes showed the same trend of increase as that of agricultural land use. Surface water body changes were strongly related to the agricultural activity in Dakhla Oasis. All wastewater was discharged consistently throughout drainage facilities and accumulated in large artificial disposal ponds or flow into natural lowland spaces [94]. The four main largest ponds were created in the northwest and north of Mut City with depths ranging from 1 to 3 m.

3.2.2. Kharga Oasis

From 1987 to 2021, the distribution of LULC in Kharga Oasis expanded from north to south and developed from west to east along with the increase in the urban and agricultural areas (Figures 4a–d and S2). The overall trends in the LULC types in Kharga Oasis were similar to those seen in Dakhla Oasis over the 35 years (Figure 6a,b). During the study period, there was a three-fold expansion in the agricultural area of Kharga Oasis, and the size of the urban area doubled. From 1987 to 2019, the agricultural land in Kharga Oasis showed a continuous trend of increase, with a slight trend of decrease seen from 2019 to 2021. Between 1987 and 2005, the agricultural and urban areas showed somewhat opposite trends in terms of change (Figure 6b). Similar to in Dakhla Oasis, this may be due to the classification of abandoned agricultural and fallow areas as urban areas. In contrast, from 2005 to 2019, these both showed trends of increase. This indicates that the urban and agricultural areas of Kharga Oasis have increased by a large extent since 2005.

The overall surface water body area showed a trend of increase, except for the trend of decrease observed in the periods 1999–2002, 2008–2011, and 2017–2021 (Figure 6b). The instability of water bodies is mainly related to the haphazard (and often illegal) exploitation of groundwater resources in Kharga Oasis, resulting in the accumulation of wastewater as surface water bodies and ponds [95].

3.2.3. Farafra Oasis

From observing the changes in the entire study area in Farafra Oasis (Figure 5i), the changes in agricultural land and urban area were found to be similar to those in both Dakhla and Kharga Oases. From 1987 to 2005, the Farafra Oasis agricultural area expanded from north to southwest (Figure 5a–d), from northeast to central from 2005, and then to the northwest in 2019 (Figure 5d–f). In 2019, a large center-pivot area appeared in the northwest of Farafra Oasis, but this area decreased in 2021 (Figure S3).

The three classes (agricultural, urban, and surface water areas) all showed an overall trend of increase over the study period (Figure 6c); this trend of increase is particularly apparent for agriculture, and urban area is a close second. Agricultural land and urban area divisions show an opposite trend of change during the period 1999–2005, then displayed a consistent trend of increase after 2005 before decreasing between 2019 and 2021.

The surface water body area showed an overall trend of increase, with a rapid increase seen from 1987 to 1996. However, the period 1996–2011 showed an overall trend of decrease, followed by a trend of increase from 2011 to 2017 and a trend of decrease from 2017 to 2021 (Figure 6c). The surface water body in Farafra Oasis contains agricultural drainage (mainly shallow drainage), water bodies that are parts of tourist attractions, and rheocrenic ambient springs [96]. The main changes in surface water bodies were not the same as those seen in the Dakhla and Kharga Oases, since the trend of decrease seen from 1995 can be attributed to the intensive development of a new type of irrigation (center-pivot) in this oasis.

The results demonstrated that the main land types of LULC in the three New Valley oases were urban area and cropland. The LULC observed in these oases showed a 35-year increase in the area of agricultural land, urban area, and surface water bodies. The largest change at the three oases seen in the study period was the increase in agriculture cover area (Figures 3–5).

The distribution of agricultural land in New Valley's oases in the study period showed a trend of increase. The urban area divisions also showed the same trend as agricultural land. The surface water bodies in the oases again showed a trend of increase, representing groundwater use indices for agricultural irrigation. Generally, the evaluation of LULC revealed that agricultural land showed spatial progressions throughout the study period.

3.3. Spatial Pattern Changes in LULC

Agricultural land expanded primarily along the perimeters of the Dakhla and Kharga Oases (Figures 7 and 8), invading the desert and changing from the mass of bare land (Figures 7–9). The second-largest change was from urban area to agricultural land (Figures 7b, 8b and 9a).

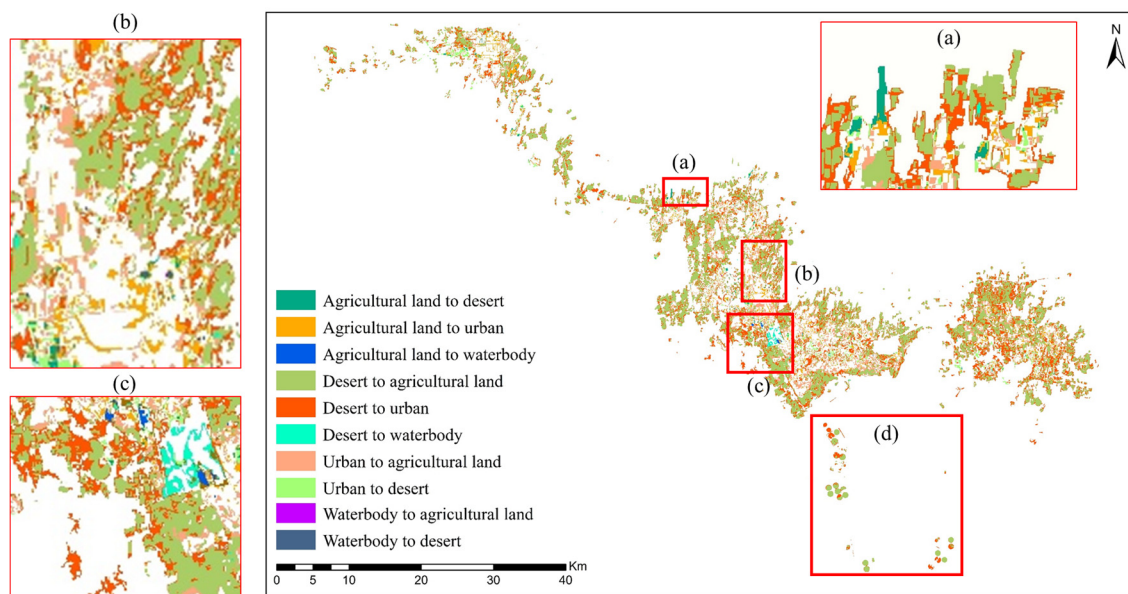


Figure 7. Dakhla Oasis LULC changes from 1986 to 2021. Regions of interest are magnified to display examples of changes from agricultural land to desert, (a) desert to agricultural land, (b) urban to agricultural land, (c) desert to water body, and (d) center-pivot agricultural land.

During the 35-year investigation, a new form of agricultural irrigation type, center-pivot (Figures 7d, 8c and 9b–d), appeared in the three oases of New Valley. Small areas of center-pivots appeared in the south of the Dakhla and Kharga Oases, whereas in Farafra large areas of center-pivots developed. This has led to the further development of the Farafra Oasis. The most important impact of such changes was on the surface water bodies.

This study indicated the proliferation and rapid change in the surface water body area (Figure 6a–c). In Dakhla Oasis, the surface water area was 0.8 km² in 1986, 2.3 km² in 2002, and 5.75 km² in 2021. In Kharga Oasis, the area was 0.4 km² in 1987, 0.8 km² in 2002, and 2.5 km² in 2021. In Farafra Oasis, the area increased from 5.3 km² in 1987 to 24.93 km² in 1995, then gradually decreased to 13.5 km² in 2011. From 2014 to 2019, the area remained at approximately 21 km² but decreased to 8 km² in 2021. This is because New Valley began to extensively develop its center-pivot irrigation system for oasis agriculture, which is recognized as an effective method to improve the distribution of water to fields [97].

The LULC transition matrix (Table 5) and LULC change maps for the 35 years (Figures 7–9) demonstrate some important spatiotemporal patterns in the three oases of New Valley. The LULC changes in the three oases exhibit many variations in land cover types, especially with regard to two classes: agricultural and urban land.

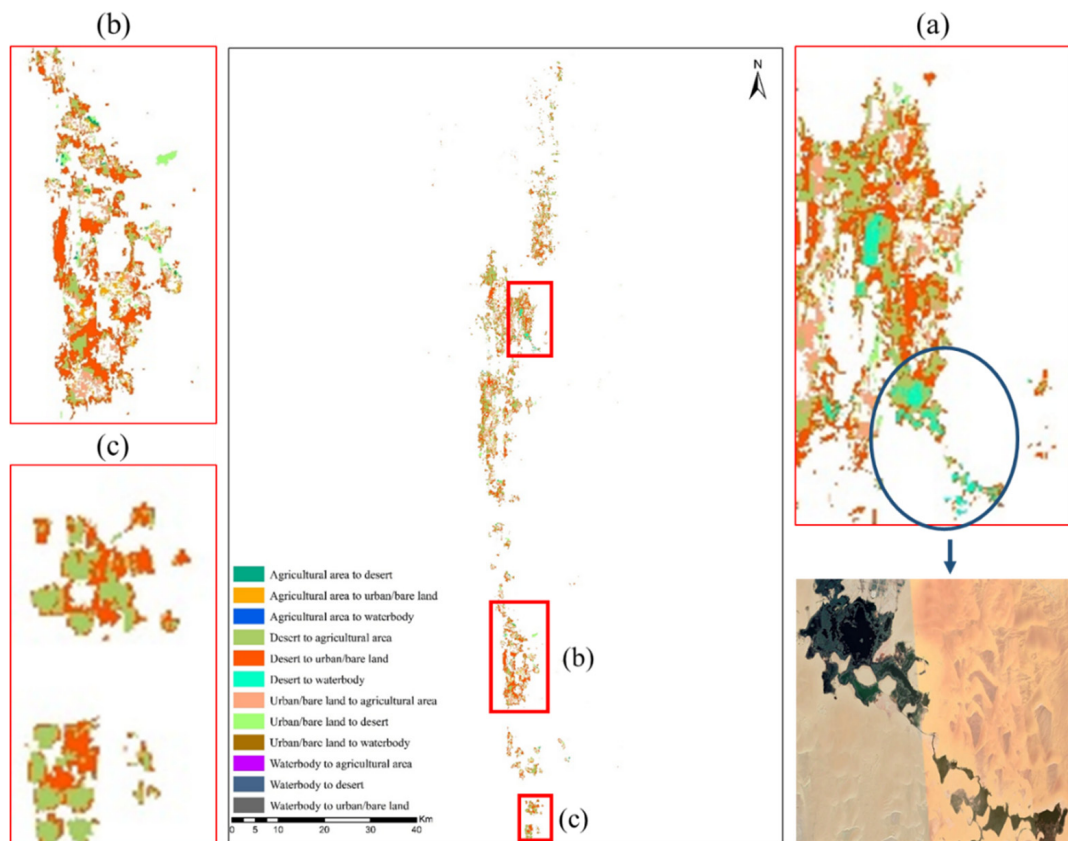


Figure 8. Kharga Oasis LULC changes from 1987 to 2021. Regions of interest are magnified to display examples of changes from agricultural land to desert; (a) desert to waterbody, (b) urban area to agricultural land and desert to urban area, and (c) center-pivot agricultural land.

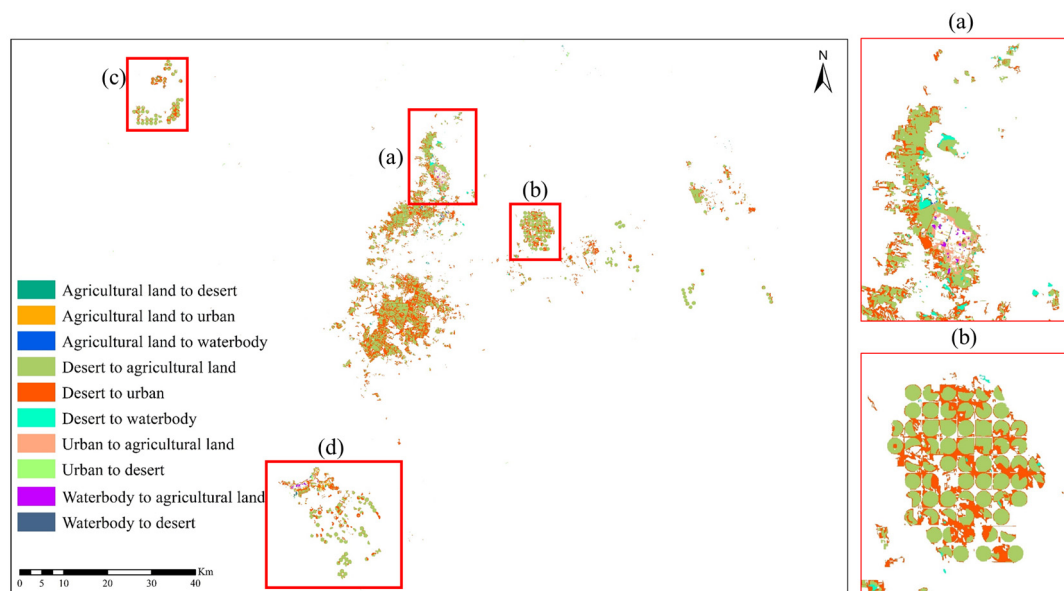


Figure 9. Farafra Oasis LULC changes from 1987 to 2021. Regions of interest are magnified to display examples of changes from agricultural area to desert; (a) desert to agricultural land, desert to waterbody, desert to urban, and (b–d) center-pivot.

Table 5. Transition matrix showing the changes in the area of each class in the three oases of New Valley during the study period (km²).

Dakhla Oasis_(km ²)				
1986–2021	Agricultural	Water	Urban	Desert
Agricultural	111.20	0.67	27.47	4.21
Water	0.05	0.94	0.10	0.08
Urban	48.70	0.84	46.18	13.90
Desert	246.87	2.86	161.90	-
Kharga Oasis_(km ²)				
1987–2021	Agricultural	Water	Urban	Desert
Agricultural	43.77	0.01	11.15	2.10
Water	0.17	0.11	0.10	0.05
Urban	36.71	0.08	38.90	11.28
Desert	86.41	2.31	120.90	-
Farafra Oasis_(km ²)				
1987–2021	Agricultural	Water	Urban	Desert
Agricultural	10.46	0.40	4.96	1.90
Water	1.71	1.466	1.42	0.75
Urban	4.10	0.26	2.62	1.90
Desert	261.60	5.80	230.30	-

3.4. Water Usage Estimation of New Valley

3.4.1. Irrigation Water Usage Estimation

The irrigation water consumption per unit value [$W_{\text{Egypt}}/A_{\text{Egypt}}$] calculated from statistical data is shown in Table 6. The lowest value found was 0.85 m³/m² in 2005 and 2011, and the highest found was 1.21 m³/m² in 2008; the average irrigation water consumption per unit value between 2002 and 2019 was 1.03 m³/m². The agricultural water consumption in 2020 and 2021 was calculated using the average irrigation water consumption per unit value between 2002 and 2019.

Table 6. Irrigation water use for per unit value [$W_{\text{Egypt}}/A_{\text{Egypt}}$] calculated from the Egypt Statistical Yearbook from 2002 to 2019.

Year	2002	2003	2004	2005	2006	2007	2008	2009	2010
Water (m ³ /m ²)	1.03	1.07	1.09	0.85	1.16	1.19	1.21	0.94	1.03
Year	2011	2012	2013	2014	2015	2016	2017	2018	2019
Water (m ³ /m ²)	0.85	0.87	1.01	1.02	0.96	1.14	1.09	1.06	1.02

The agricultural land area data obtained from the LULC results every three years were deemed insufficient to quantify the overall water consumption of the past 20 years for reasonable comparison with the quantitative results for groundwater storage extraction. For this reason, we used the Landsat 7 Collection 1 Tier 1 8-Day NDVI Composite combined with the threshold method to efficiently extract the total available cultivated land [$A_{\text{New Valley oases}}$] of the three oases along with East Oweinat in New Valley from 2002 to 2021 (Figure 10a). The results obtained using the threshold method and the OBIA (for LULC) method showed high correlations of 0.92, 0.93, and 0.95 for agricultural areas in the Dakhla, Kharga, and Farafra oases, respectively (Figure 11). Combining the irrigation water consumption per unit value [$W_{\text{Egypt}}/A_{\text{Egypt}}$] with the total agricultural area [$A_{\text{New Valley oases}}$] (see Equation (1)), the calculated changes in agricultural irrigation water consumption (per year) from 2002 to 2021 [$W_{\text{New Valley oases}}$] are shown in Figure 10b.

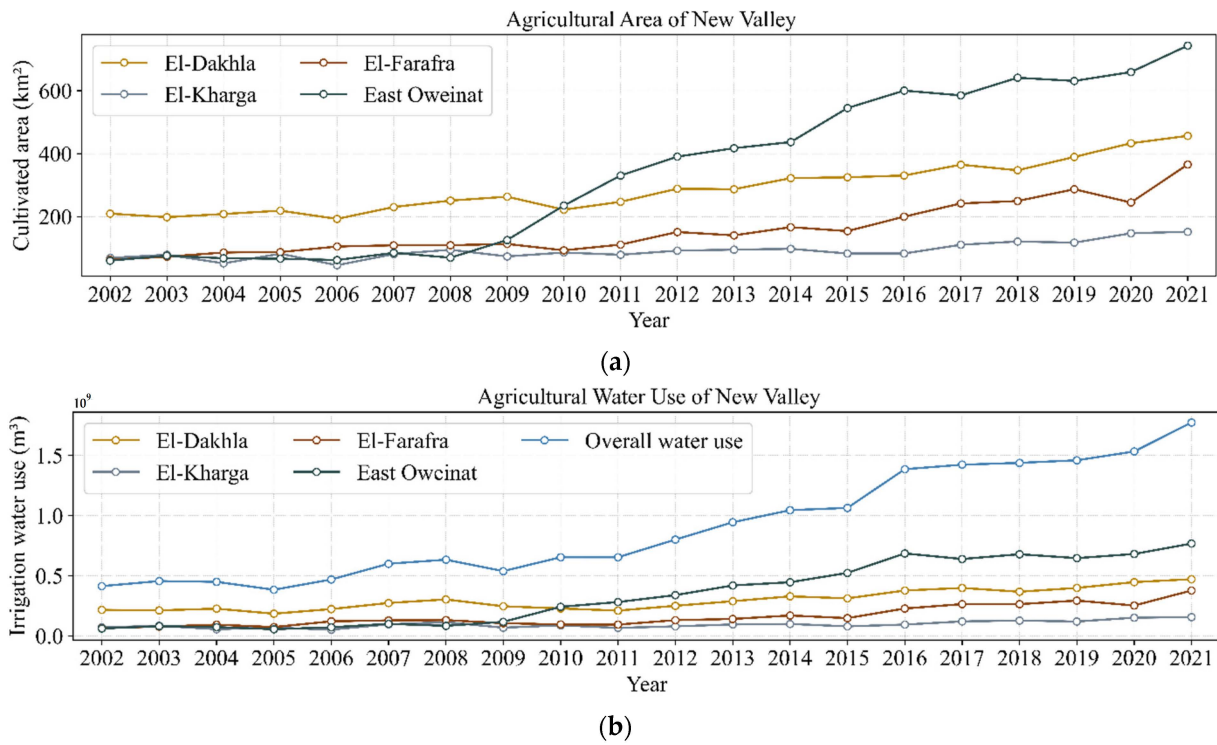


Figure 10. (a) Cultivated area of three oases and East Oweinat of New Valley; (b) irrigation water use estimation for the cultivated area of the three oases and East Oweinat in New Valley.

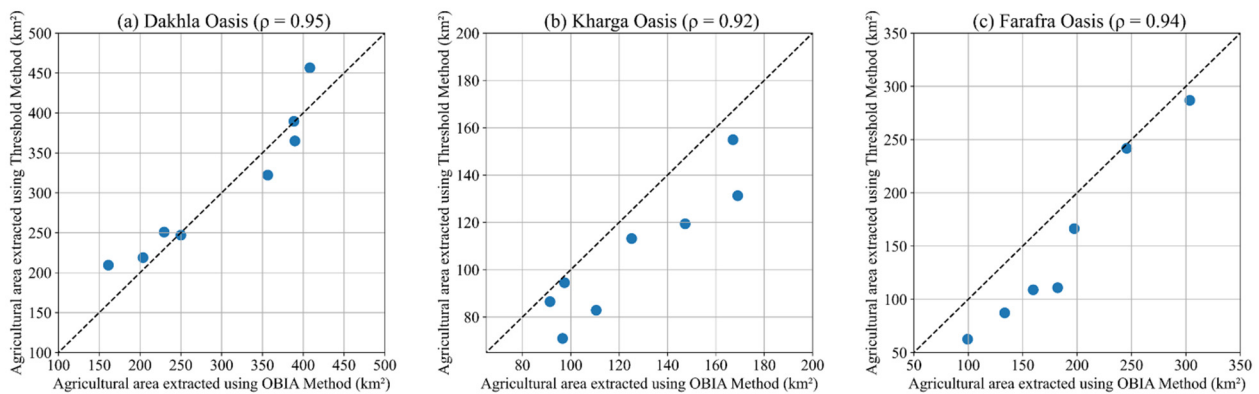


Figure 11. Correlation between agricultural area extracted using the OBIA (LULC) method and that extracted using the threshold method from 2002 to 2021 in the three oases of New Valley, (a) Dakhla Oasis, (b) Kharga Oasis, (c) Farafra Oasis.

The results indicated that the area of cultivated land has expanded in each oasis of the study area (Figure 10a). With the increase in agricultural area, the overall water consumed for irrigation in the study area showed a tendency of continuous growth (Figure 10b). Combining all three oases with East Oweinat, the total water demand increased from $4.1 \times 10^8 \text{ m}^3$ in 2002 to $17.7 \times 10^8 \text{ m}^3$ in 2021. According to the estimations, New Valley's overall irrigation water usage increased about three-fold. The overall irrigation water use from 2002 to 2021 was 18.1 km^3 . The results of the water consumption estimation indicate that agricultural water demand has been increasing since 2005 (Figure 10b). Compared with other years, the increase in agricultural irrigation water consumption reached the highest values in 2011–2014, and the increase in 2014–2017 was lower than the previous range.

3.4.2. Domestic Water Usage Estimation

In Egypt, in 1999, the amount of available water per capita for all purposes was $900 \text{ m}^3/\text{yr}$, but this is estimated to drop to $670 \text{ m}^3/\text{yr}$ in 2017 and $536 \text{ m}^3/\text{yr}$ in 2025 [98]. The actual water consumption per capita may be lower than the estimated value [99]. Here, we use $98.6 \text{ m}^3/\text{yr}/\text{capita}$ [98] for calculating the domestic water consumption for New Valley, Egypt. The results show that the domestic water needs from 2002 to 2021 increased along with the population increase. The overall domestic water use from 2002 to 2021 was calculated as 0.52 km^3 . The population development of New Valley is described below in Section 4.1.

3.5. Extraction of Groundwater Changes

Higher spatial variations can be observed in CSR because of the higher spatial resolution (0.25°) than the JPL (0.5°) solutions (Figure 12a,b). Changes in Equivalent Water Height (EWH) from two GRACE mascon solutions (CSR and JPL) between the GRACE investigation period (April 2002 and July 2021), expressed in centimeters, are presented in Figure 13.

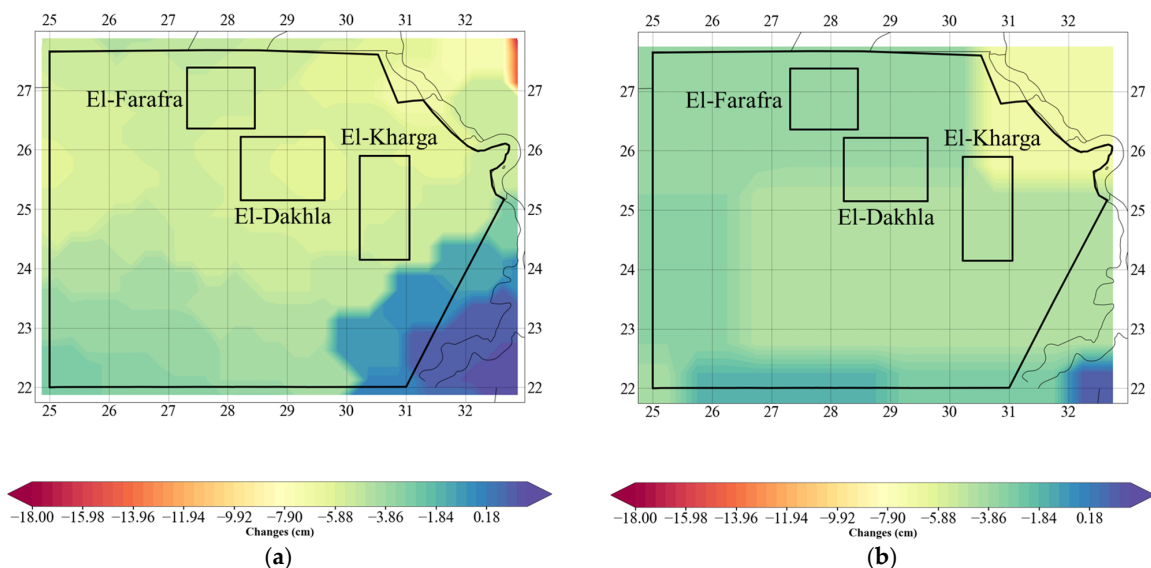


Figure 12. The spatial changes of ΔGWS between April 2002 and July 2021 were extracted from two GRACE mascon solutions; (a) CSR-GRACE/GRACE-FO mascon solution and (b) JPL-GRACE/GRACE-FO mascon solution.

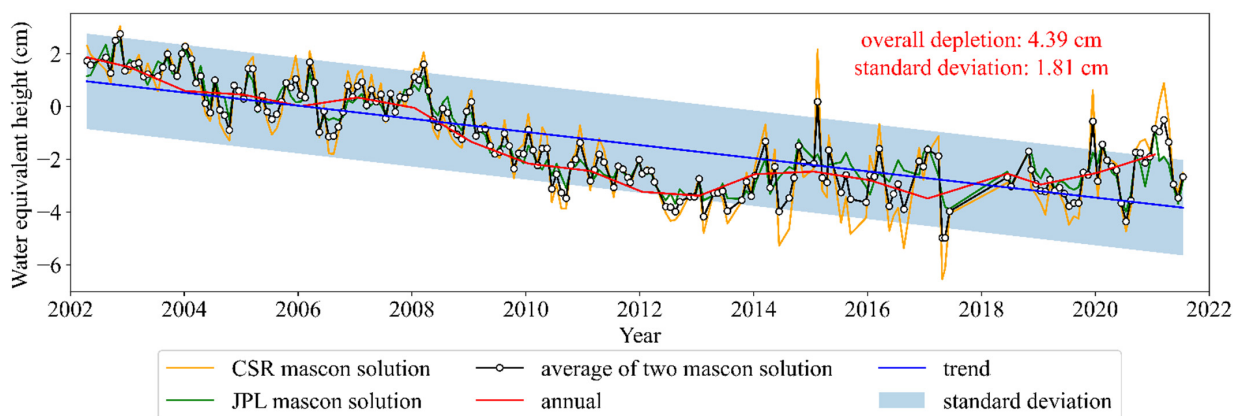


Figure 13. ΔGWS time series from two GRACE mascon solutions (shown in Figure 10) and its arithmetic mean during the study period in New Valley. Also shown (blue line) is the linear trend in ΔGWS for the entire investigated period (April 2002–July 2021).

The groundwater storage changes of New Valley were extracted from the combination of GRACE CSR and JPL mascon solutions, expressed in cm, between April 2002 and July 2021 (GRACE investigated period), along with associated inter-annual trends obtained using a 199-month averaging window (Figure 13). The extraction results show a trend of decrease from 2002 to 2021. The overall depletion thickness was calculated to be 4.39 cm (standard deviation of 1.8105). The NSAS New Valley experienced a depletion of $19.36 \pm 7.96 \text{ km}^3$ ($0.97 \pm 0.39 \text{ km}^3/\text{yr}$) during the investigated period (Figure 13).

Figure 13 shows the secular trend images for GWS estimates generated from CSR mascon (Figure 12a); JPL mascon (Figure 12b); and the average of the two solutions over NSAS, New Valley. Figure 13 indicates that the NSAS, New Valley, experienced average negative ($-2.2 \text{ mm}/\text{yr}$) GWS trends over the investigated period.

The spatial distributions of GWS trends slightly varied with the source of the GRACE mascon data. For example, in the case of the CSR mascon solutions (Figure 12a), for areas witnessing a negative ($-2.4 \text{ mm}/\text{yr}$) GWS trend over the New Valley, the JPL mascon-derived trends (Figure 2b) were slightly (9%) lower than mean trends, which witnessed a uniform negative ($-1.98 \text{ mm}/\text{yr}$) GWS trend. This is probably related to the approaches used to generate the TWS products. For example, the JPL mascon was generated from 3° spherical caps, and the CSR mascon was generated from a 1° hexagon (in Section 2.2.3).

A time series of ΔGWS was analyzed (Figure 14). According to the change detection analysis, there are two trends over the entire period. One was a downward trend in the first 12 years (April 2002–November 2013) of the investigation, with NSAS in New Valley experiencing depletion of $1.18 \pm 0.42 \text{ km}^3/\text{yr}$. The other was a flat or weak augmentation trend following this over the remaining eight years (December 2013–July 2021). The groundwater storage of NSAS in New Valley might experience a non-significant trend of increasing ΔGWS ($0.38 \pm 0.23 \text{ km}^3/\text{yr}$) during this period (Figures 13 and 14).

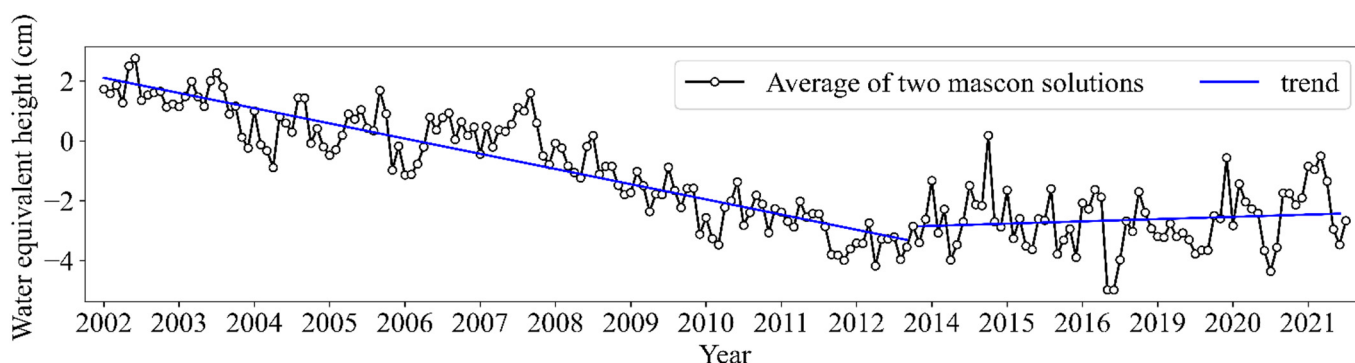


Figure 14. Change detection analysis in ΔGWS (average of two GRACE mascon solutions). Blue lines represent two different trends for the periods April 2002 to November 2013 and December 2013 to July 2021.

4. Discussion

4.1. Population Growth and Production Changes

The population of the New Valley Governorate grew from 160,281 in 2002 [69] to 257,772 in 2021 [3], increasing by approximately 60% (Figure 15a). Even today, the population of the study area is still increasing. The population of Egypt is also increasing.

Figure 15c shows the development index for the total agricultural and food production in Egypt, which was extracted from the Egypt Statistical Yearbook.

Generally, the growing population demands more land for basic living needs, such as food and housing. With the growth in the population in the three oases in New Valley, food production has increased correspondingly. It is an aspect that the agricultural land has increased as the population of the oasis residents and the residents' demand; however, the most important reason is the land reclamation driven by the Egyptian government and agribusiness companies [7].

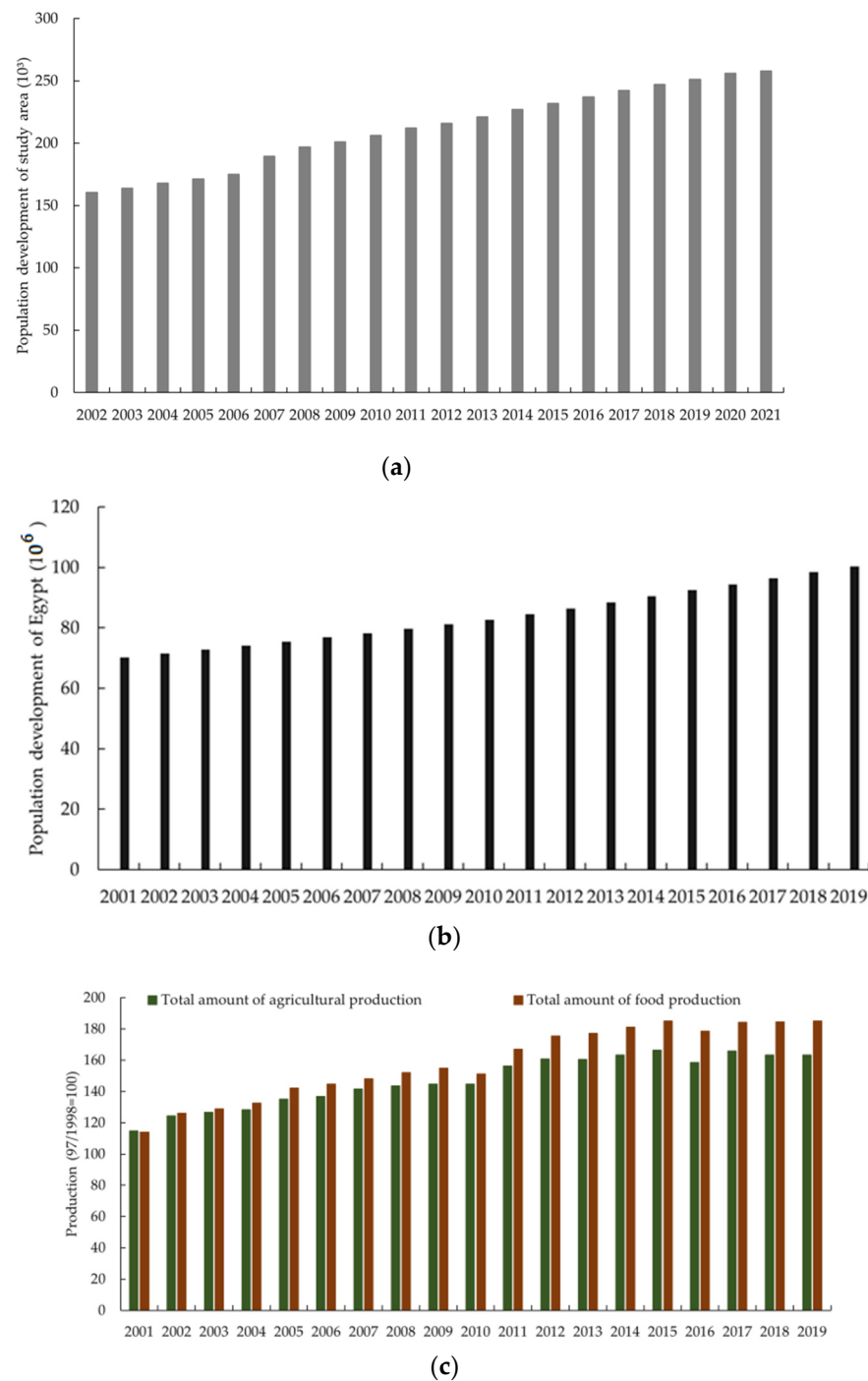


Figure 15. (a) Total population development of the study area; (b) total population development of Egypt; (c) development index for the total amount of agricultural and food production in Egypt (2001–2019); source: Egypt Statistical Yearbook [2,3,69,70].

4.2. LULC Changes Analysis

In 1960, the Egyptian government proposed the “New Valley Project”, which was intended to cultivate new cropland and re-cultivate the ancient cropland, which had been gradually abandoned [100]. This project covered about 458,000 km², extending across the Kharga, Dakhla, and Farafra Oases. The urban area in the Dakhla and Kharga Oases has been relatively stable in recent years; it has undergone small expansions, but there have been no significant overall changes. A detailed analysis of the transition of LULC classes (Table 5) revealed that human–environment interactions have shaped the LULC

dynamics of the study area. For example, contrary to what is commonly believed, the urban area in all three oases of the New Valley has experienced conversion into other land cover types (e.g., agricultural land) (Table 5). This somewhat unconventional land-use transition may be linked with local land use habits, which are predominantly influenced by environmental disturbances and climate change [101,102]. In the desert areas, the decreased rainfall and increased evapotranspiration demand in the oases may lead to water scarcity and land degradation. These problems might be prevented by modifying agricultural practices (including irrigation and drainage techniques) and applying plant rotation. The progressive surface water body area changes in the three oases represent a response to the usage of groundwater [94,95], which might also be used as an indicator of groundwater use. Galal and Darwish (2020) [94] also indicate that the formation of wastewater can mainly be attributed to the rapid expansion of agricultural areas, which has placed the study area under substantial stress.

4.3. Water Usage Analysis

One of the main purposes of our study is to determine whether the amount of water extracted is consistent with the actual water used for agricultural and domestic purposes.

In 2011, there was a decrease in the per unit value irrigation water usage (Table 6). The specific reasons for this can be traced back to the Egyptian revolution that took place in 2011. This revolution was a remarkable event in the modern history of Egypt. Labor protests across Egypt reached unprecedented scales [103]. All industries were affected so much that the GDP levels were forecast to be the lowest in recent years [104].

Due to its extremely arid climate, with an annual precipitation close to 0 mm, the water used for irrigation in the study area is solely dependent on groundwater from the Nubian Sandstone Aquifer System. Changes in GWS can be attributed to climatic and anthropogenic factors. No correlation between GW changes and atmospheric hydrological fluxes (P, ET, PET) [49] can be seen. The human factors involved are described in Section 4.1: the human-related ongoing increase in water consumption in the study area heightens the competition between human needs (anthropogenic activities) and natural resources, supporting the idea that there is a strong correlation between increased cultivated area and groundwater extraction. From the results of this study, it can be seen that groundwater usage changed due to increased levels of human activities related to irrigation, which led to a decrease in groundwater.

The annual average depletion rate of GWS in New Valley was calculated to be $1.18 \pm 0.42 \text{ km}^3/\text{yr}$ for 2002 to 2013 and $0.97 \pm 0.39 \text{ km}^3/\text{yr}$ for 2002 to 2021. The overall amount of water used in New Valley for domestic purposes and irrigation was calculated as 18.62 km^3 . The groundwater storage changes in New Valley were extracted using GRACE and estimated to be $19.36 \pm 7.96 \text{ km}^3$. Thus, the water usage for domestic and agricultural purposes is comparable with the rate of groundwater depletion. As a result, in this study we analyzed the long-term (April 2002–November 2013, December 2013–July 2021) time series of monthly GWS calculated from GRACE observations over New Valley using breakpoint detection. The reported groundwater extraction rate, which is $19.36 \pm 7.96 \text{ km}^3$ ($0.97 \pm 0.39 \text{ km}^3/\text{yr}$), is consistent with the LULC-derived (irrigation and domestic) water use trends which is 18.62 km^3 ($0.93 \text{ km}^3/\text{yr}$) over the entire investigated period. The overall irrigation water use from 2002 to 2021 was 18.1 km^3 —as the primary water consumption sector, agricultural land consumes more than 90% of the available water resources.

5. Conclusions

This study attempted to quantify the water consumption in a hyper-arid region—New Valley, Egypt—using two different approaches: LULC based on optical remote sensing data and groundwater storage changes based on Gravity Recovery Climate Experiment (GRACE) satellite data.

Land use land cover (LULC) distribution development was mapped in three main oases in New Valley, Egypt. The results show that rate of change in LULC in the three

cases was increased. Deserts have increasingly been turned into agricultural land. The agricultural area and irrigation water use increased continuously from 2002 to 2021 because of the land reclamation. The progressive surface water body area changes, which might indicate groundwater use.

As the primary water consumption sector, agricultural land consumes more than 90% of the available water resources. The population and food production also increased. The total irrigation water was calculated as 18.1 km³, whereas the domestic water was calculated as 0.52 km³ from 2002 to 2021 in New Valley, Egypt. The overall water use was calculated as 18.62 km³, which is 0.93 km³/yr on average.

GRACE satellite data for groundwater storage changes were calculated as 19.36 ± 7.96 km³ (1.01 ± 0.42 km³/yr) in the study area from 2002 to 2021.

The actual water use of New Valley and changes in the groundwater storage in this region were quantified for the first time and compared with the results of prior research. The trend of increasing groundwater storage seen since 2014 could be attributed to the increased irrigation efficiency, which will be further investigated in future studies. Such information will be vital in the management and mitigation plans for this arid region.

Supplementary Materials: The following supporting information can be downloaded at: <https://www.mdpi.com/article/10.3390/rs14112608/s1>.

Author Contributions: Conceptualization, A.H.; formal analysis, A.H.; funding acquisition, E.I.; methodology, A.H. and X.W.; supervision, W.Y. and A.K.; validation, A.H.; writing—original draft, A.H. All authors have read and agreed to the published version of the manuscript.

Funding: This research was funded by the research project “Development of the sustainable underground water use in the water-scarce societies in North Africa” (MEXT/JSPS KAKENHI Grant Number, Project JP17H16026).

Data Availability Statement: Publicly available datasets were analyzed in this study. These datasets can be found in Reference.

Conflicts of Interest: The author declares that there is no conflict of interest. The funder has no role in research design; in data collection, analysis, or interpretation; in the writing of the manuscript; or in the decision to publish the results.

References

- Kato, H.; Iwasaki, E. *Rashda: The Birth and Growth of an Egyptian Oasis Village*; BRILL: Leiden, The Netherlands, 2016; ISBN 978-90-04-31739-0.
- Egypt Statistical Yearbook. 2004. Available online: https://www.capmas.gov.eg/Pages/Publications.aspx?page_id=5104&YearID=23543&Year=23567 (accessed on 1 March 2022).
- Egypt Statistical Yearbook. 2021. Available online: https://www.capmas.gov.eg/Pages/StaticPages.aspx?page_id=5034 (accessed on 1 March 2022).
- Population Growth (Annual %)|Data. Available online: <https://data.worldbank.org/indicator/SP.POP.GROW> (accessed on 1 March 2022).
- AbouKorin, A. Sustainability Requirements of Desert Development in Egypt: The Case of New Valley Region. *Minia J. Eng. Technol. (MJET)* **2002**, *1*, 1–12.
- New Valley: Profile*; IDSC Information and Decision Support Centre: Cairo, Egypt, 1997.
- Nour, S.E. Grabbing from below: A Study of Land Reclamation in Egypt. *Rev. Afr. Political Econ.* **2019**, *46*, 549–566. [CrossRef]
- Ozdogan, M.; Yang, Y.; Allez, G.; Cervantes, C. Remote Sensing of Irrigated Agriculture: Opportunities and Challenges. *Remote Sens.* **2010**, *2*, 2274–2304. [CrossRef]
- Transboundary Aquifers of the World. 2015. Available online: http://ihp-wins.unesco.org/layers/tba_map2015:geonode:tba_map2015 (accessed on 4 February 2022).
- Watanabe, M.; Sugimura, T.; Kamei, H. Interpretation of Characteristics of the Land Use Change Based on Chronological Satellite Imageries of Kharga Oasis, Western Desert, Egypt. *J. Remote Sens. Soc. Jpn.* **2014**, *34*, 356–366. [CrossRef]
- Ahmed, M.; Abdelmohsen, K. Quantifying Modern Recharge and Depletion Rates of the Nubian Aquifer in Egypt. *Surv. Geophys.* **2018**, *39*, 729–751. [CrossRef]
- KATO, H.; Elbeih, S.; Iwasaki, E.; Sefelnasr, A.; Shalaby, A.; Zaghoul, E. The Relationship between Groundwater, Landuse, and Demography in Dakhla Oasis, Egypt. *E-J. Asian Netw. GIS-Based Hist. Stud.* **2014**, *2*, 3–10.

13. Shalaby, A.; Khedr, H.S. Remote Sensing and GIS for Land Use/Land Cover Change Detection in Dakhla Oasis. In *Sustainable Water Solutions in the Western Desert, Egypt: Dakhla Oasis*; Iwasaki, E., Negm, A.M., Elbeih, S.F., Eds.; Earth and Environmental Sciences Library; Springer International Publishing: Cham, Switzerland, 2021; pp. 145–159, ISBN 978-3-030-64005-7.
14. Iwasaki, E.; Shalaby, A.; Elbeih, S.F.; Khedr, H.S. Development of Land Use and Groundwater in Rashda Village (Dakhla Oasis), 1960s–2018. In *Sustainable Water Solutions in the Western Desert, Egypt: Dakhla Oasis*; Iwasaki, E., Negm, A.M., Elbeih, S.F., Eds.; Earth and Environmental Sciences Library; Springer International Publishing: Cham, Switzerland, 2021; pp. 219–240, ISBN 978-3-030-64005-7.
15. Kato, H.; Kimura, R.; Elbeih, S.F.; Iwasaki, E.; Zaghoul, E.A. Land Use Change and Crop Rotation Analysis of a Government Well District in Rashda Village – Dakhla Oasis, Egypt Based on Satellite Data. *Egypt. J. Remote Sens. Space Sci.* **2012**, *15*, 185–195. [[CrossRef](#)]
16. Abdel Kawy, W.A.M.; Abou El-Magd, I.H. Use of Satellite Data and GIS for Assessing the Agricultural Potentiality of the Soils South Farafra Oasis, Western Desert, Egypt. *Arab. J. Geosci.* **2013**, *6*, 2299–2311. [[CrossRef](#)]
17. Global Water Resources: Vulnerability from Climate Change and Population Growth. Available online: <https://www.science.org/doi/full/10.1126/science.289.5477.284> (accessed on 1 April 2022).
18. Jalilvand, E.; Tajrishy, M.; Ghazi Zadeh Hashemi, S.A.; Brocca, L. Quantification of Irrigation Water Using Remote Sensing of Soil Moisture in a Semi-Arid Region. *Remote Sens. Environ.* **2019**, *231*, 111226. [[CrossRef](#)]
19. Serra, P.; Salvati, L.; Queralt, E.; Pin, C.; Gonzalez, O.; Pons, X. Estimating Water Consumption and Irrigation Requirements in a Long-Established Mediterranean Rural Community by Remote Sensing and Field Data. *Irrig. Drain.* **2016**, *65*, 578–588. [[CrossRef](#)]
20. Zhao, W.; Chang, X.; Chang, X.; Zhang, D.; Liu, B.; Du, J.; Lin, P. Estimating Water Consumption Based on Meta-Analysis and MODIS Data for an Oasis Region in Northwestern China. *Agric. Water Manag.* **2018**, *208*, 478–489. [[CrossRef](#)]
21. Rozenstein, O.; Haymann, N.; Kaplan, G.; Tanny, J. Estimating Cotton Water Consumption Using a Time Series of Sentinel-2 Imagery. *Agric. Water Manag.* **2018**, *207*, 44–52. [[CrossRef](#)]
22. Fleming, K.; Martinec, Z.; Hagedoorn, J. Geoid Displacement about Greenland Resulting from Past and Present-Day Mass Changes in the Greenland Ice Sheet. *Geophys. Res. Lett.* **2004**, *31*, L06617. [[CrossRef](#)]
23. Flury, J. Ice Mass Balance and Ice Dynamics from Satellite Gravity Missions. *Earth Moon Planet* **2004**, *94*, 83–91. [[CrossRef](#)]
24. Wunsch, J. Oceanic and Soil Moisture Contributions to Seasonal Polar Motion. *J. Geodyn.* **2002**, *33*, 269–280. [[CrossRef](#)]
25. Swenson, S.C.; Milly, P.C.D. Climate Model Biases in Seasonality of Continental Water Storage Revealed by Satellite Gravimetry. *Water Resour. Res.* **2006**, *42*, W03201. [[CrossRef](#)]
26. The Potential for Satellite-Based Monitoring of Groundwater Storage Changes Using GRACE: The High Plains Aquifer, Central US—ScienceDirect. Available online: <https://www.sciencedirect.com/science/article/pii/S0022169402000604> (accessed on 6 February 2022).
27. Frappart, F.; Ramillien, G. Monitoring Groundwater Storage Changes Using the Gravity Recovery and Climate Experiment (GRACE) Satellite Mission: A Review. *Remote Sens.* **2018**, *10*, 829. [[CrossRef](#)]
28. Liu, X.; Hu, L.; Sun, K.; Yang, Z.; Sun, J.; Yin, W. Improved Understanding of Groundwater Storage Changes under the Influence of River Basin Governance in Northwestern China Using GRACE Data. *Remote Sens.* **2021**, *13*, 2672. [[CrossRef](#)]
29. Scanlon, B.R.; Longuevergne, L.; Long, D. Ground Referencing GRACE Satellite Estimates of Groundwater Storage Changes in the California Central Valley, USA. *Water Resour. Res.* **2012**, *48*, W04520. [[CrossRef](#)]
30. Wu, Q.; Si, B.; He, H.; Wu, P. Determining Regional-Scale Groundwater Recharge with GRACE and GLDAS. *Remote Sens.* **2019**, *11*, 154. [[CrossRef](#)]
31. Thomas, B.F.; Famiglietti, J.S. Identifying Climate-Induced Groundwater Depletion in GRACE Observations. *Sci. Rep.* **2019**, *9*, 4124. [[CrossRef](#)] [[PubMed](#)]
32. Melati, M.D.; Fleischmann, A.S.; Fan, F.M.; Paiva, R.C.; Athayde, G.B. Estimates of Groundwater Depletion under Extreme Drought in the Brazilian Semi-Arid Region Using GRACE Satellite Data: Application for a Small-Scale Aquifer. *Hydrogeol. J.* **2019**, *27*, 2789–2802. [[CrossRef](#)]
33. Munier, S.; Becker, M.; Maisongrande, P.; Cazenave, A. Using GRACE to Detect Groundwater Storage Variations: The Cases of Canning Basin and Guarani Aquifer System. *Int. Water Technol. J.* **2012**, *2*, 2–13.
34. Vasco, D.W.; Farr, T.G.; Jeanne, P.; Doughty, C.; Nico, P. Satellite-Based Monitoring of Groundwater Depletion in California’s Central Valley. *Sci. Rep.* **2019**, *9*, 16053. [[CrossRef](#)]
35. Singh, L.; Saravanan, S. Satellite-Derived GRACE Groundwater Storage Variation in Complex Aquifer System in India. *Sustain. Water Resour. Manag.* **2020**, *6*, 1–15. [[CrossRef](#)]
36. Shukla, M.; Maurya, V.; Dwivedi, R. Groundwater Monitoring Using GRACE Mission. *Int. Arch. Photogramm. Remote Sens. Spat. Inf. Sci.* **2021**, *43*, B3-2021. [[CrossRef](#)]
37. Singh, A.K.; Jasrotia, A.S.; Taloor, A.K.; Kotlia, B.S.; Kumar, V.; Roy, S.; Ray, P.K.C.; Singh, K.K.; Singh, A.K.; Sharma, A.K. Estimation of Quantitative Measures of Total Water Storage Variation from GRACE and GLDAS-NOAH Satellites Using Geospatial Technology. *Quat. Int.* **2017**, *444*, 191–200. [[CrossRef](#)]
38. Zhong, Y.; Zhong, M.; Feng, W.; Zhang, Z.; Shen, Y.; Wu, D. Groundwater Depletion in the West Liaohe River Basin, China and Its Implications Revealed by GRACE and in Situ Measurements. *Remote Sens.* **2018**, *10*, 493. [[CrossRef](#)]
39. Neves, M.C.; Nunes, L.M.; Monteiro, J.P. Evaluation of GRACE Data for Water Resource Management in Iberia: A Case Study of Groundwater Storage Monitoring in the Algarve Region. *J. Hydrol. Reg. Stud.* **2020**, *32*, 100734. [[CrossRef](#)]

40. Bhanja, S.N.; Zhang, X.; Wang, J. Estimating Long-Term Groundwater Storage and Its Controlling Factors in Alberta, Canada. *Hydrol. Earth Syst. Sci.* **2018**, *22*, 6241–6255. [[CrossRef](#)]
41. Saber, M.; Alhinai, S.; Al Barwani, A.; AL-Saidi, A.; Kantoush, S.A.; Habib, E.; Borrok, D.M. Satellite-Based Estimates of Groundwater Storage Changes at the Najd Aquifers in Oman. In *Water Resources in Arid Areas: The Way Forward*; Springer: Berlin/Heidelberg, Germany, 2017; pp. 155–169.
42. Ouma, Y.O.; Aballa, D.O.; Marinda, D.O.; Tateishi, R.; Hahn, M. Use of GRACE Time-Variable Data and GLDAS-LSM for Estimating Groundwater Storage Variability at Small Basin Scales: A Case Study of the Nzoia River Basin. *Int. J. Remote Sens.* **2015**, *36*, 5707–5736. [[CrossRef](#)]
43. Feng, W.; Shum, C.K.; Zhong, M.; Pan, Y. Groundwater Storage Changes in China from Satellite Gravity: An Overview. *Remote Sens.* **2018**, *10*, 674. [[CrossRef](#)]
44. Liesch, T.; Ohmer, M. Comparison of GRACE Data and Groundwater Levels for the Assessment of Groundwater Depletion in Jordan. *Hydrogeol. J.* **2016**, *24*, 1547–1563. [[CrossRef](#)]
45. Lo, M.-H.; Famiglietti, J.S.; Reager, J.T.; Rodell, M.; Swenson, S.; Wu, W.-Y. GRACE-Based Estimates of Global Groundwater Depletion. *Terr. Water Cycle Clim. Change Nat. Hum.-Induc. Impacts* **2016**, *221*, 137.
46. Rodell, M.; Chen, J.; Kato, H.; Famiglietti, J.S.; Nigro, J.; Wilson, C.R. Estimating Groundwater Storage Changes in the Mississippi River Basin (USA) Using GRACE. *Hydrogeol. J.* **2007**, *15*, 159–166. [[CrossRef](#)]
47. Humphrey, V.; Gudmundsson, L.; Seneviratne, S.I. Assessing Global Water Storage Variability from GRACE: Trends, Seasonal Cycle, Subseasonal Anomalies and Extremes. *Surv. Geophys.* **2016**, *37*, 357–395. [[CrossRef](#)]
48. Mohamed, A.; Sultan, M.; Ahmed, M.; Yan, E.; Ahmed, E. Aquifer Recharge, Depletion, and Connectivity: Inferences from GRACE, Land Surface Models, and Geochemical and Geophysical Data. *GSA Bull.* **2017**, *129*, 534–546. [[CrossRef](#)]
49. Frappart, F. Groundwater Storage Changes in the Major North African Transboundary Aquifer Systems during the GRACE Era (2003–2016). *Water* **2020**, *12*, 2669. [[CrossRef](#)]
50. Robinson, C.A.; Werwer, A.; El-Baz, F.; El-Shazly, M.; Fritch, T.; Kusky, T. The Nubian Aquifer in Southwest Egypt. *Hydrogeol. J.* **2007**, *15*, 33–45. [[CrossRef](#)]
51. Dabous, A.A.; Osmond, J.K. Uranium Isotopic Study of Artesian and Pluvial Contributions to the Nubian Aquifer, Western Desert, Egypt. *J. Hydrol.* **2001**, *243*, 242–253. [[CrossRef](#)]
52. Kimura, R.; Kato, H.; Iwasaki, E. Cultivation Features Using Meteorological and Satellite Data from 2001 to 2010 in Dakhla Oasis, Egypt. *J. Water Resour. Prot.* **2015**, *07*, 209–218. [[CrossRef](#)]
53. Nada, A.A. Evaluation of Environmental Isotopic and Salinar Composition of Groundwater in Oases of the Western Desert, Egypt. *Isot. Environ. Health Stud.* **1995**, *31*, 117–124. [[CrossRef](#)]
54. The Nubian Aquifer in Southwest Egypt | SpringerLink. Available online: <https://link.springer.com/article/10.1007/s10040-006-0091-7> (accessed on 16 March 2022).
55. Kimura, R.; Iwasaki, E.; Matsuoka, N. Analysis of the Recent Agricultural Situation of Dakhla Oasis, Egypt, Using Meteorological and Satellite Data. *Remote Sens.* **2020**, *12*, 1264. [[CrossRef](#)]
56. Summary of Current Radiometric Calibration Coefficients for Landsat MSS, TM, ETM+, and EO-1 ALI Sensors—ScienceDirect. Available online: <https://www.sciencedirect.com/science/article/pii/S0034425709000169> (accessed on 29 March 2022).
57. Kriegler, F.J.; Malila, W.A.; Nalepka, R.F.; Richardson, W. Preprocessing Transformations and Their Effects on Multispectral Recognition. *Remote Sens. Environ.* **1969**, *VI*, 97.
58. Greicius, T. Grace Mission. Available online: http://www.nasa.gov/mission_pages/Grace/index.html (accessed on 6 February 2022).
59. Tapley, B.; Bettadpur, S.; Watkins, M.; Reigber, C. The Gravity Recovery and Climate Experiment: Mission Overview and Early Results. *Geophys. Res. Lett.* **2004**, *31*, 4. [[CrossRef](#)]
60. Kim, J. *Simulation Study of a Low-Low Satellite-to-Satellite Tracking Mission*; The University of Texas at Austin: Austin, TX, USA, 2000; p. 291.
61. Kornfeld, R.P.; Arnold, B.W.; Gross, M.A.; Dahya, N.T.; Klipstein, W.M.; Gath, P.F.; Bettadpur, S. GRACE-FO: The Gravity Recovery and Climate Experiment Follow-On Mission. *J. Spacecr. Rocket.* **2019**, *56*, 931–951. [[CrossRef](#)]
62. Landerer, F.W.; Flechtner, F.M.; Save, H.; Webb, F.H.; Bandikova, T.; Bertiger, W.I.; Bettadpur, S.V.; Byun, S.H.; Dahle, C.; Dobslaw, H.; et al. Extending the Global Mass Change Data Record: GRACE Follow-On Instrument and Science Data Performance. *Geophys. Res. Lett.* **2020**, *47*, e2020GL088306. [[CrossRef](#)]
63. Hasan, E.; Tarhule, A. Comparison of Decadal Water Storage Trends from Common GRACE Releases (RL05, RL06) Using Spatial Diagnostics and a Modified Triple Collocation Approach. *J. Hydrol. X* **2021**, *13*, 100108. [[CrossRef](#)]
64. Save, H.; Bettadpur, S.; Tapley, B.D. High Resolution CSR GRACE RL05 Mascons. *J. Geophys. Res. Solid Earth* **2016**, *121*, 7547–7569. [[CrossRef](#)]
65. Save, H. CSR GRACE and GRACE-FO RL06 Mascon Solutions V02. *Mascon Solut.* **2020**, *12*, 24. [[CrossRef](#)]
66. Watkins, M.M.; Wiese, D.N.; Yuan, D.-N.; Boening, C.; Landerer, F.W. Improved Methods for Observing Earth’s Time Variable Mass Distribution with GRACE Using Spherical Cap Mascons. *J. Geophys. Res. Solid Earth* **2015**, *120*, 2648–2671. [[CrossRef](#)]
67. Wiese, D.N.; Landerer, F.W.; Watkins, M.M. Quantifying and Reducing Leakage Errors in the JPL RL05M GRACE Mascon Solution. *Water Resour. Res.* **2016**, *52*, 7490–7502. [[CrossRef](#)]
68. Wiese, D.N.; Yuan, D.-N.; Boening, C.; Landerer, F.W.; Watkins, M.M. *JPL GRACE Mascon Ocean, Ice, and Hydrology Equivalent Water Height Release 06 Coastal Resolution Improvement (CRI) Filtered Version 1.0. Ver. 1.0.*; PO.DAAC: Pasadena, CA, USA, 2018.

69. Egypt Statistical Yearbook. 2012. Available online: https://www.capmas.gov.eg/Pages/Publications.aspx?page_id=5104&YearID=23543&Year=23563 (accessed on 1 March 2022).
70. Egypt Statistical Yearbook. GHDx. 2017. Available online: <http://ghdx.healthdata.org/record/egypt-statistical-yearbook-2017> (accessed on 24 February 2022).
71. Baatz, M.; Schäpe, A. Multiresolution Segmentation: An Optimization Approach for High Quality Multi-Scale Image Segmentation. *Comput. Sci.* **2000**, *38*, 12–23.
72. Flanders, D.; Hall-Beyer, M.; Pereverzoff, J. Preliminary Evaluation of ECognition Object-Based Software for Cut Block Delineation and Feature Extraction. *Can. J. Remote Sens.* **2003**, *29*, 441–452. [[CrossRef](#)]
73. Abhir, H.; Bhalerao, B.S. *Multiresolution Image Segmentation*; The University of Warwick: Coventry, UK, 1991.
74. Seidl, T. Nearest Neighbor Classification. In *Encyclopedia of Database Systems*; LIU, L., ÖZSU, M.T., Eds.; Springer: Boston, MA, USA, 2009; pp. 1885–1890, ISBN 978-0-387-39940-9.
75. Platt, R.V.; Rapoza, L. An Evaluation of an Object-Oriented Paradigm for Land Use/Land Cover Classification. *Prof. Geogr.* **2008**, *60*, 87–100. [[CrossRef](#)]
76. Willhauck, G. *Comparison of Object Oriented Classification Techniques and Standard Image Analysis for the Use of Change Detection between SPOT Multispectral Satellite Images and Aerial Photos*; IAPRS: Amsterdam, The Netherlands, 2000; Volume 33, pp. 35–42.
77. Hossain, M.D.; Chen, D. Segmentation for Object-Based Image Analysis (OBIA): A Review of Algorithms and Challenges from Remote Sensing Perspective. *ISPRS J. Photogramm. Remote Sens.* **2019**, *150*, 115–134. [[CrossRef](#)]
78. Goodchild, M.F. GIScience, Geography, Form, and Process. *Ann. Assoc. Am. Geogr.* **2004**, *94*, 709–714. [[CrossRef](#)]
79. Goodchild, M.F. Geographical Information Science. *Int. J. Geogr. Inf. Syst.* **1992**, *6*, 31–45. [[CrossRef](#)]
80. Yu, Q.; Gong, P.; Clinton, N.; Biging, G.; Kelly, M.; Schirokauer, D. Object-Based Detailed Vegetation Classification with Airborne High Spatial Resolution Remote Sensing Imagery. *Photogramm. Eng. Remote Sens.* **2006**, *72*, 799–811. [[CrossRef](#)]
81. Câmara, G.; Souza, R.C.M.; Freitas, U.M.; Garrido, J. Spring: Integrating Remote Sensing and Gis by Object-Oriented Data Modelling. *Comput. Graph.* **1996**, *20*, 395–403. [[CrossRef](#)]
82. Wu, J. Hierarchy and Scaling: Extrapolating Information along a Scaling Ladder. *Can. J. Remote Sens.* **1999**, *25*, 367–380. [[CrossRef](#)]
83. Hay, G.J.; Marceau, D.J.; Dubé, P.; Bouchard, A. A Multiscale Framework for Landscape Analysis: Object-Specific Analysis and Upscaling. *Landsc. Ecol.* **2001**, *16*, 471–490. [[CrossRef](#)]
84. Burnett, C.; Blaschke, T. A Multi-Scale Segmentation/Object Relationship Modelling Methodology for Landscape Analysis. *Ecol. Model.* **2003**, *168*, 233–249. [[CrossRef](#)]
85. Alqurashi, A.F.; Kumar, L.; Sinha, P. Urban Land Cover Change Modelling Using Time-Series Satellite Images: A Case Study of Urban Growth in Five Cities of Saudi Arabia. *Remote Sens.* **2016**, *8*, 838. [[CrossRef](#)]
86. A New Approach for Land Cover Classification and Change Analysis: Integrating Backdating and an Object-Based Method—ScienceDirect. Available online: <https://www.sciencedirect.com/science/article/pii/S003442571630058X?via%3Dihub> (accessed on 14 February 2022).
87. Rodell, M.; Velicogna, I.; Famiglietti, J.S. Satellite-Based Estimates of Groundwater Depletion in India. *Nature* **2009**, *460*, 999–1002. [[CrossRef](#)] [[PubMed](#)]
88. Famiglietti, J.S.; Lo, M.; Ho, S.L.; Bethune, J.; Anderson, K.J.; Syed, T.H.; Swenson, S.C.; de Linage, C.R.; Rodell, M. Satellites Measure Recent Rates of Groundwater Depletion in California’s Central Valley. *Geophys. Res. Lett.* **2011**, *38*. [[CrossRef](#)]
89. Quantifying Renewable Groundwater Stress with GRACE—Richey—2015—Water Resources Research—Wiley Online Library. Available online: <https://agupubs.onlinelibrary.wiley.com/doi/full/10.1002/2015WR017349> (accessed on 7 February 2022).
90. Thomas, B.F.; Caineta, J.; Nanteza, J. Global Assessment of Groundwater Sustainability Based On Storage Anomalies. *Geophys. Res. Lett.* **2017**, *44*, 11445. [[CrossRef](#)]
91. Shamsudduha, M.; Taylor, R.G.; Longuevergne, L. Monitoring Groundwater Storage Changes in the Highly Seasonal Humid Tropics: Validation of GRACE Measurements in the Bengal Basin. *Water Resour. Res.* **2012**, *48*, W02508. [[CrossRef](#)]
92. Shao, Y.; Fraedrich, K.; Ishizuka, M. Modelling Soil Moisture in Hyper-Arid Conditions. *Bound.-Layer Meteorol.* **2021**, *179*, 169–186. [[CrossRef](#)]
93. Sakumura, C.; Bettadpur, S.; Bruinsma, S. Ensemble Prediction and Intercomparison Analysis of GRACE Time-Variable Gravity Field Models. *Geophys. Res. Lett.* **2014**, *41*, 1389–1397. [[CrossRef](#)]
94. Galal, W.F.; Darwish, M. Geoenvironmental Assessment of the Mut Wastewater Ponds in the Dakhla Oasis, Egypt. *Geocarto Int.* **2020**, 1–13. [[CrossRef](#)]
95. Darwish, M.; Galal, W. Spatiotemporal Effects of Wastewater Ponds from a Geoenvironmental Perspective in the Kharga Region, Egypt. *Prog. Phys. Geogr.* **2019**, *44*, 376–397. [[CrossRef](#)]
96. Wolowski, K.; Saber, A.; Cantonati, M. Euglenoids from the El Farafra Oasis (Western Desert, Egypt). *Pol. Bot. J.* **2017**, *62*. [[CrossRef](#)]
97. Texas Crop Circles from Space. Available online: <https://climate.nasa.gov/news/729/texas-crop-circles-from-space> (accessed on 20 February 2022).
98. Ministry of the Environment. Available online: https://www.env.go.jp/earth/coop/coop/document/c_report/egypt_h16/english/pdf/000.pdf (accessed on 2 March 2022).
99. DARWISH Hosam Water Scarcity in the Middle East and North Africa: A Focus on Egypt. *Middle East Rev.* **2020**, *7*, 6–13. [[CrossRef](#)]

100. Degens, E.T. Project New Valley. *Eng. Sci.* **1961**, *25*, 20–23.
101. Dale, V.H. The Relationship Between Land-Use Change and Climate Change. *Ecol. Appl.* **1997**, *7*, 753–769. [[CrossRef](#)]
102. Kurukulasuriya, P.; Rosenthal, S. *Climate Change and Agriculture: A Review of Impacts and Adaptations*; World Bank: Washington, DC, USA, 2013.
103. Sharp, J.M. *Egypt: The January 25 Revolution and Implications for US Foreign Policy*; Diane Publishing: Collingdale, PA, USA, 2011; pp. 45–89.
104. Abdou, D. The Egyptian Revolution and Post Socio-Economic IMPACT. *Top. Middle East. Afr. Econ.* **2013**, *15*, 92.